

Forecasting and control in overlapping generations model: chaos stabilization via artificial intelligence

T.A. Alexeeva^a, Q.B. Diep^b, N.V. Kuznetsov^{1c,d}, T.N. Mokaev^c, I. Zelinka^b

^a*St. Petersburg School of Physics, Mathematics and Computer Science, HSE University,
194100 St. Petersburg, Kantemirovskaya ul., 3, Russia*

^b*Department of Computer Science, Faculty of Electrical Engineering and Computer Science, VŠB-TUO,
17.listopadu 2172/15, 708 00 Ostrava-Poruba, Czech Republic*

^c*Faculty of Mathematics and Mechanics, St. Petersburg State University, 198504 Peterhof, St. Petersburg, Russia*

^d*Institute for Problems in Mechanical Engineering RAS, 199178 St. Petersburg, V.O., Bolshoj pr., 61, Russia*

Abstract

Irregular, especially chaotic, behavior is often undesirable for economic processes because it presents challenges for predicting their dynamics. In this situation, control of such a process by its mathematical model can be used to suppress chaotic behavior and to transit the system from irregular to regular dynamics.

In this paper, we have constructed an overlapping generations model with a control function. By applying evolutionary algorithms we showed that in the absence of control, both regular and irregular behavior (periodic and chaotic) could be observed in this model. We then used the synthesis of control by the Pyragas control method with two control parameters to solve the problem of controlling the irregular behavior of the model. We solved a number of optimization problems applying evolutionary algorithms to select control parameters in order to ensure stability of periodic orbits. We compared qualitative and quantitative characteristics of the model's dynamics before and after applying control and verified the results obtained using simulation.

We thus demonstrated that artificial intelligence technologies (in particular, evolutionary algorithms) combined with the Pyragas control method are well suited for in-depth analysis and stabilization of irregular dynamics in the model considered in this paper.

Keywords: overlapping generations (OLG) model, nonlinear dynamics, forecasting, control, chaos, stabilization, optimization, artificial intelligence, evolutionary algorithms

1. Introduction

Currently the world economy develops in conditions of complexity, uncertainty and unpredictability related to technology transformation, changes in the economic structure, as well as a number of exogenous challenges, including climatic, energy, and epidemiological cataclysms [1–3]. These challenges stimulated posing of new problems both in the real economy and in economic science, which led to conceptual shifts in the testing of hypotheses about the functioning of economic systems, construction of the mathematical models as well as analysis and forecasting their dynamics [4–11]. Economists need to know how models can impact in the real world and they often focus not only on forecasts but also on model inference, on understanding and interpretation the model parameters. Nevertheless, economic and fiscal policies conceived by governments, central banks, and other decision-makers heavily depend on economic forecasts, in particular during times of economic, societal, and natural turmoils, policy makers must support their decisions by

¹Corr. author email nkuznetsov239@gmail.com

providing and communicating explanations for the action taken. Therefore, they are interested in the economic implications associated with model predictions. The success of mathematical modeling significantly depends on the ability to obtain rich information about economic activity and uncover complex economic relationships that could be useful to forecast the economy in normal time, and also to identify early signals of problems in markets before crises [12]. In order to get a more complete picture of the state of the economy and its future behavior, researchers increasingly rely on both theoretical concepts and various types of economic data, including detailed micro-data and big data. This allows studying behavior of complex, large scale, nonlinear, models with a large number of variables or parameters, as well as forecasting the dynamics of economic processes. Given such features of modern models, special technologies adapted to powerful computing resources are required to analyze them, forecast, and verify the predictions. In this regard, it is difficult to offer a more suitable tool than methods based on artificial intelligence (AI) technologies, since AI algorithms can handle severe nonlinearities, are easy to dynamically scale to large state spaces and thousands computer nodes [12–17]. There is a vast literature [12, 13, 18–35] that provides impressive examples of applying various AI technologies, such as machine learning (ML) methods, like support vector machines, decision trees, random forests; deep learning (DL), including reinforcement learning; semantic web technologies, involving natural language processing; and evolutionary algorithms (EAs) [36–41], to solve a wide spectrum of the practice-focused and theoretical problems in the economy. Nonlinear behavior of the modern models presents special challenges to the accuracy of forecasting, both in the short and medium to long run. If nonlinearities are present in the model, irregular dynamics and complex limit behavior could arise that may manifest themselves as unstable regimes or chaos. Chaotic behavior in a model of an economic system may lead to unpredictable events, complicate analytical and numerical study of the model, finding acceptable values of the model parameters, and hinder the accuracy of forecasts over longer horizons, thus undermining the predictive power of the model [42, 43]. This is undesirable from the point of view of policy makers aiming to stabilize aggregate fluctuations. Numerous papers [43–66] attempted to explain such features of economic data as irregular and erratic microeconomic and macroeconomic fluctuations, financial and credit crises, structural changes, and overlapping waves of economic development from the point of view of chaos theory. A common theme in this literature is explaining the complexity and unpredictable behavior of economic processes by nonlinear dynamical models. Trajectories in such models, starting somewhere in the phase space, can be attracted not only to a stable stationary point or a periodic cycle, but to an irregular invariant set, including chaotic attractor [67–70]. Additional complexity of the dynamics can be also associated with various unstable orbits embedded into the chaotic attractor of the dynamical system. If the model that describes particular economic phenomenon exhibits such complex dynamics, its forecasting and control becomes a very important problem to be solved. In this regard, the usage of AI technologies in combination with the classical control methods allows making significant progress in determining the qualitative properties of the model dynamics, including revealing of regular and irregular (periodic and chaotic) regimes, fine-tuning of the possible initial points, optimization of the model parameters, and stabilization of unstable orbits by using control procedures [71–73].

In this paper, we demonstrate the effectiveness of applying the numerical and analytic approach grounded on EAs and the Pyragas control method [74, 75] to investigate and forecasting the irregular dynamics of macroeconomic processes using one of overlapping generations (OLG) models as an example. A pioneering OLG model, which was developed by Nobel laureates Paul Samuelson (1970) and Peter Diamond (2010) in [76, 77], is a representative of a very important class of low dimensional economic models with optimizing agents that are used to analyze the basic intertemporal choice of consumption and saving and the dynamic consequences of these choices, as well as to explore dynamics of education, retirement, capital accumulation, public policies, inflation,

fiscal policies, etc. (see, e.g. [43, 43, 78–95])². Despite being low dimensional, OLG models are shown to exhibit a wide range of complex behaviors – saddle-path converging toward the steady state [78], cycles [79], divergence [79], sunspot equilibria [85], multiple equilibria [43], and chaos [79]. In this paper, we derive a two period OLG model with production and endogenous labor choice which is represented by a discrete-time dynamical model arising from solutions of economic agents’ dynamic optimization problems: for consumers and firms. The model is deterministic, where agents exist in an environment of perfect foresight and have exact information about the values of the model parameters and the trajectories of solutions in the phase space along which the dynamics of the model evolves. Even with parameter values that imply existence of a chaotic regime, starting from specific initial conditions could lead to switching to a trajectory with predictable dynamics by applying control, modeled as time varying government spending. In the absence of control, the model can behave both regularly and irregularly, including periodically and chaotically. We show how such a model could be successfully studied by consecutive application of EAs and the Pyragas method. To this end, we chose the most powerful EA methods, i.e. differential evolution (DE) [36] and the self-organized migration algorithm (SOMA) [37]. To suppress the chaotic regime of the model’s dynamics, we started by applying EAs to overcome a complex fractional-power nonlinearity of the model to find the suspected unstable periodic orbits embedded into the attractor. To refine these trajectories, we used the Pyragas method, then synthesized a time-delayed feedback control and found out its parameters by solving a particular optimization problem using EAs in such a way that the periodic trajectory became locally stable. Last but not least, using EAs and computational abilities of a supercomputer, we also solved an optimal control problem of maximizing the basin of attraction of the stabilized UPO, and fine-tuning of the possible initial points from which the state of the system is attracted to the specified trajectory. Thereby, all the principal stages of the examination of the limiting dynamics of the OLG model were performed using the EAs. Our result shows that even for low-dimensional nonlinear models in the case of chaotic behavior, it is sometimes critical to use EAs combined with the computing power of supercomputers to be able to solve particular control and optimal control problems, as well as forecasting problems.

2. The model

OLG models are a useful theoretical concept that allows one to construct economic theories, introduce and interpret various effects of economic policies, and understand how the economic system functions given the finite life cycle of economic agents. First, these models allow us to explicitly consider life-cycle issues and demographic trends, including education and pension systems, and to study variety of problems associated with financing and reforming them, as well as to estimate the effect of population ageing on pension reforms and government fiscal policy [91, 92]. Second, these models introduce a natural heterogeneity of agents belonging to different cohorts, which makes it possible to speak of intergenerational transfers (education as a transfer from employed population to the young, pensions as transfers from employed population to the elderly), to investigate mechanisms of trade between generations [78], and to estimate both short-run transitory and long-run dynamic macroeconomic effects of tax reforms [88, 89]. Third, these models naturally introduce incomplete markets as the agents do not have access to markets that existed before they were born and cannot trade in markets that open after their death. This creates an opportunity to deviate

²The reason interest in OLG models has not faded almost a century after [76] is well described in [86] dedicated to the 50th anniversary of publication of Samuelson’s paper: “Like Mona Lisa’s enigmatic smile, the mysterious welfare properties of the overlapping generations model are, to a significant extent, responsible for its popularity—along with the many economic issues it has illuminated in the last half-century.”

from the fundamental theorems of welfare economics [96], and can lead to such nontrivial economic phenomena with complex dynamics as sunspots, indeterminacy, over-accumulation of capital, etc (see, e.g. [97–99]). The OLG models thus are of special interest for study, because they present a complicated environment with varied dynamics, including stationary states, cycles of all periods, and even chaotic dynamics [95].

Here we derive a new OLG model developing the ideas proposed in [100], who considered a two-period OLG model with two types of economic agents: firms and households (i.e. consumers). Economic agents live for two periods. In every period t , there are two consumer cohorts (of size 1)³: the one born at t (young) and the one born at $t - 1$ (old). Consumers maximize their welfare by solving a dynamic optimization problem subject to the budget constraint and determine work hours and savings. Consumers work only in period 1 but consume in both periods. In period t , the young born at t work, providing labor hours l_t , and consume c_t^t . Here a superscript t denotes cohort, or time of birth, and a subscript is physical time. They consume a single good which also could be saved and turned into capital k_t , which will be used for production in the next period $t + 1$. In the second period of their life, the agents cannot work, and could only consume their savings with interest. Profit maximizing firms use labor and capital to produce a single good used for consumption and investment. In contrast to [100], our model takes full account of the old cohort's consumption. Additionally, [100] takes one of the fundamental model parameters – γ (labor elasticity), to be the control. This amounts to a new agent with different preferences appearing at each point in time when the controller changes γ . While agents' preferences could be stochastic, they cannot be controlled by any government or a social planner. In our model, we introduce government spending, which is an external non-fundamental variable. Government spending is financed by proportional labor tax, and is used as a control variable in a chaotic regime.

2.1. Utility side

Let $c_t = c_t^t$ is consumption of young at period t , $c_{t+1} = c_{t+1}^t$ is consumption of young at period $t + 1$ when they will be old. The only meaningful decision, therefore, is that of young agents, who at time t must make an optimal choice of their consumption while young (c_t^t), consumption when old (c_{t+1}^t), and working hours when young (l_t). The optimal behavior is represented in the optimization problem – the *consumer problem*

$$\max U_t = u_1(c_t^t) + u_2(c_{t+1}^t) - v(l_t), \quad (1)$$

s.t.

$$c_t^t + k_t = (1 - \tau_t) w_t l_t, \quad (2)$$

$$c_{t+1}^t = R_{t+1} k_t,$$

where $u_1(c_t^t)$ is the utility of consuming while young, $u_2(c_{t+1}^t)$ the (future) utility of consuming when old, and $v(l_t)$ disutility of labor. In the first period, the *budget constraint* (2) says that consumption c_t^t plus capital (k_t) equals the income of the young, given by their labor income $w_t l_t$ net of proportional taxes (for example, profits tax) with rate τ_t . Here w_t is the real wage rate, R_{t+1} is the gross real interest rate. In the second period of their life (physical time $t + 1$), the agents born at t consume their savings with interest. Non-negativity constraints form part of the model.

Plugging in both constraints into the utility function, we get the following problem:

$$\max_{k_t, l_t} U_t = u_1((1 - \tau_t) w_t l_t - k_t) + u_2(R_{t+1} k_t) - v(l_t), \quad (3)$$

³But we could also think that there is only one person in every generation.

which produces the following first order conditions (FOCs):

$$\begin{aligned}\frac{\partial U_t}{\partial k_t} &= 0 : -u'_1(c_t^t) + R_{t+1}u'_2(c_{t+1}^t) = 0, \\ \frac{\partial U_t}{\partial l_t} &= 0 : (1 - \tau_t) w_t \cdot u'_1(c_t^t) - v'(l_t) = 0.\end{aligned}\tag{4}$$

From the second equation, we see that

$$(1 - \tau_t) w_t = \frac{v'(l_t)}{u'_1(c_t^t)},\tag{5}$$

and from the first that

$$R_{t+1} = \frac{u'_1(c_t^t)}{u'_2(c_{t+1}^t)}.\tag{6}$$

Plugging both into the budget constraint (2), we get

$$\begin{aligned}c_t^t + k_t &= c_t^t + \frac{c_{t+1}^t}{R_{t+1}} = c_t^t + c_{t+1}^t \frac{u'_1(c_t^t)}{u'_2(c_{t+1}^t)} = \\ &= (1 - \tau_t) w_t l_t = \frac{v'(l_t) l_t}{u'_1(c_t^t)}, \\ c_t^t u'_1(c_t^t) + c_{t+1}^t u'_2(c_{t+1}^t) - v'(l_t) l_t &= 0,\end{aligned}\tag{7}$$

Using the same functional forms as in [100]

$$\begin{aligned}u_1(c_t^t) &= \frac{1}{\theta} (c_t^t)^\theta, \quad 0 < \theta < 1 \\ u_2(c_{t+1}^t) &= \frac{1}{\alpha} (c_{t+1}^t)^\alpha, \quad 0 < \alpha < 1 \\ v(c_t^t) &= \frac{1}{\gamma} (c_t^t)^\gamma, \quad \gamma > 1,\end{aligned}\tag{8}$$

we get the first equation of our model

$$c_{t+1}^t = \left(l_t^\gamma - (c_t^t)^\theta \right)^{\frac{1}{\alpha}}.\tag{9}$$

2.2. Technological side

The second equation of our model can be obtained as the *resource constraint*. In [100] production is modeled using the Leontieff type production linear function, which determines the amount of output y_t given inputs l_t (labor) and k_{t-1} (capital):

$$y_t = \min(al_t, bk_{t-1}).\tag{10}$$

We use the another way. We introduce the Cobb-Douglas production technology as a nonlinear function:

$$y_t = l_t^\beta k_{t-1}^{1-\beta}.\tag{11}$$

The *profit* maximization function will give us the following *firms' problem*:

$$\max_{k_t, l_t} \Pi_t = l_t^\beta k_{t-1}^{1-\beta} - w_t l_t - R_t k_{t-1},\tag{12}$$

which produces the following FOCs:

$$\begin{aligned}\frac{\partial \Pi_t}{\partial l_t} &= 0 : \beta \frac{y_t}{l_t} - w_t = 0, \\ \frac{\partial \Pi_t}{\partial k_{t-1}} &= 0 : (1 - \beta) \frac{y_t}{k_{t-1}} - R_t = 0.\end{aligned}\tag{13}$$

From equations (13), we obtain the following

$$w_t = \beta \frac{y_t}{l_t},\tag{14}$$

$$R_t = (1 - \beta) \frac{y_t}{k_{t-1}},\tag{15}$$

therefore,

$$\frac{w_t}{R_t} = \frac{\beta}{(1 - \beta)} \frac{k_{t-1}}{l_t}.\tag{16}$$

Note that the production functions (10) and (11) are thresholds of the CES function. Now, we come back to the Leontieff production function (10). At time t the inputs to production are labor of the time t young, l_t , and the capital saved by the agents who were born at time $t - 1$ and thus are old at time t , k_{t-1} . As the constant a determines only the coefficient of proportionality between the labor input and output, it is normalized to 1. The Leontieff production technology implies that the firm maximizing its profits will use its inputs in a fixed proportion, so that

$$y_t = l_t = b k_{t-1},\tag{17}$$

therefore,

$$\frac{k_{t-1}}{l_t} = \frac{1}{b}.\tag{18}$$

Thus, we can say that relation between of the real wage rate w_t and the gross real interest rate R_t is defined as the limit state of CES function through the Cobb-Douglas production technology (16). Hence, using the same ratio of $\frac{w_t}{R_t}$ as in the Cobb-Douglas production technology case (16) and $\frac{k_{t-1}}{l_t}$ ratio as in the Leontieff technology case (18), we get

$$\frac{R_t}{w_t} = b \frac{(1 - \beta)}{\beta}.\tag{19}$$

Moreover, we can use relations from Cobb-Douglas case (15), taking into account (17) and (19), then

$$R_t = (1 - \beta) \frac{y_t}{k_{t-1}} = (1 - \beta) \frac{b k_{t-1}}{k_{t-1}} = (1 - \beta) b,\tag{20}$$

and

$$w_t = \beta \frac{y_t}{l_t} = \beta \frac{l_t}{l_t} = \beta.\tag{21}$$

In order to get the second equation of the OLG model, we then need to determine how is the good produced at time t , y_t , allocated. The total amount of the good produced is split between consumption of the young alive at t , c_t^t , savings of the young alive at t , k_t , consumption of the old alive at t , c_t^{t-1} , and the *government spending* g_t . The government spending is financed through the proportional tax on the young, and the amount collected equals $\tau_t w_t l_t$. The government spending isn't used for anything productive and doesn't contribute to the utility of consumers, that's why

it does not appear anywhere in the problem of young consumers (1). The only purpose of the government spending g_t in this model is to provide a *control variable*.

We rectify the resource constraint in model [100], to take into account not only the consumption of the young in the current period, but also the consumption of the old in both periods (i.e., when they were young). Therefore, to obtain the second equation of our model, we now could write *resource constraint*

$$l_t = y_t = k_t + c_t^t + c_t^{t-1} + g_t = bk_{t-1}. \quad (22)$$

From (22), taking into account (17), we obtain the following

$$k_{t-1} = y_{t-1} - c_{t-1}^{t-1} - c_{t-1}^{t-2} - g_{t-1}, \quad (23)$$

and

$$l_t = b(l_{t-1} - c_{t-1}^{t-1} - c_{t-1}^{t-2} - g_{t-1}). \quad (24)$$

Moving forward one period, we obtain the second equation that characterizes the dynamics of the OLG model

$$l_{t+1} = b(l_t - c_t^t - c_t^{t-1} - g_t). \quad (25)$$

However, we need to eliminate c_t^{t-1} from the equation, because it is the consumption of old cohort. Moving backward one period in the second equation from (4) and taking into account (17) and (20), we obtain

$$c_t^{t-1} = (1 - \beta)l_t. \quad (26)$$

Finally, plugging last relation into (25), we get the OLG model with control function g_t

$$\begin{cases} c_{t+1}^t = \left(l_t^\gamma - (c_t^t)^\theta\right)^{1/\alpha}, \\ l_{t+1} = b(\beta l_t - c_t^t - g_t). \end{cases} \quad (27)$$

Equations (27) represent a nonlinear dynamical model of two equations in two variables, l_t and c_t^t , with one control variable g_t included additively. Thus, the government spending is

$$g_t = \tau_t w_t l_t = \tau_t \beta l_t. \quad (28)$$

So the government spending is a share of today's wage bills, and thus of today's output. Note that the government spending in the previous period, $g_{t-1} > 0$, enter with the negative sign in the equation for the current output $y_t = l_t$. This is because past period's government spending forced the agents born at time $t - 1$ (current old) to reduce both their first period consumption, c_{t-1}^{t-1} , and the amount of capital they bought with their savings, k_{t-1} . With less capital, the Leontieff technology forces the firms in period t to demand less labor and produce less output.

2.3. Control

From an economic point of view, interventions in the model aimed at controlling chaotic dynamics can only be carried out by way of introducing a variable that could be intentionally controlled, for example, taxes, government spending, government consumption or investment, etc. Therefore, in our model, we introduce government spending (non-fundamental variable), which is used as a control variable. Thus, we avoid the problem arising in the model in [100] if labor elasticity γ is chosen as the control parameter. The parameter γ is fundamental and cannot be changed, therefore it is not suitable for control.

We would have a control function as $g_t = K(l_t - l_{t-m})$ (for periodic orbit with period m). Due to $g_t = \tau_t \beta l_t$ we can consider the proportional taxes with rate τ_t as $\tau_t = \frac{K}{\beta} \left(1 - \frac{l_{t-m}}{l_t}\right)$. One note of

caution. As is stated previously, the government spending is financed through taxes on the labor income of the young. Therefore, it cannot be larger than $w_t l_t$ or smaller than 0, which is condition that needs to be checked during simulations. Also, given that the technology is Leontieff, the wage rate w_t and the interest rate R_{t+1} cannot be determined from the optimal conditions of the firm, as is usually done in the economic literature. They are, to a large degree, arbitrary. It might therefore be advisable to use a Cobb-Douglas production function (11) instead, which will allow to introduce wage and interest rate in a non-arbitrary manner, while complicating the equations.

3. Dynamics of the OLG model

3.1. Analysis of the uncontrolled OLG model

Our OLG model with respect to variables (c_t, l_t) ⁴ and control g_t is described by the following two-dimensional map $\varphi : \mathbb{R}^2 \rightarrow \mathbb{R}^2$, where:

$$\varphi(c_t, l_t) = ((l_t^\gamma - c_t^\theta)^{1/\alpha}, b(\beta l_t - c_t - g_t)), \quad (29)$$

and $0 < \alpha, \theta < 1$, $0 < \beta \leq 1$, $\gamma \geq 1$, $b > 1$ are parameters. This map generates the following discrete-time dynamical model

$$\begin{cases} c_{t+1} = (l_t^\gamma - c_t^\theta)^{1/\alpha}, \\ l_{t+1} = b(\beta l_t - c_t - g_t), \end{cases} \quad t \in \mathbb{Z}_+, \quad (30)$$

which describes complex behavior of agents in conditions of economic equilibrium – a situation when supply and demand in all markets are balanced.

First, we consider the case $g_t = 0$. To calculate the equilibria, we must solve a nonlinear system defined by

$$\begin{cases} c_t = (l_t^\gamma - c_t^\theta)^{1/\alpha}, \\ l_t = b(\beta l_t - c_t). \end{cases}$$

There are two equilibria in this model: the first one $E_1 = (0, 0)$ is trivial and always locally unstable, while the second one, $E_2 = (c_\star > 0, l_\star > 1)$, cannot even be calculated explicitly.

For the sake of simplicity, let us consider a special case

$$\theta = \alpha$$

and using the following change of variables $c_t := c_t^{1/\alpha}$, $l_t := l_t$ and parameter $\lambda = 1/\alpha$ rewrite initial map (29) in the following form:

$$\psi(c_t, l_t) = (l_t^\gamma - c_t, b(\beta l_t - c_t^\lambda)), \quad (31)$$

with the following constraints:

$$\lambda > 1, \quad 0 < \beta < 1, \quad \gamma > 1, \quad b > 1. \quad (32)$$

For the dynamical model, generated by map (31), i.e.

$$\begin{cases} c_{t+1} = l_t^\gamma - c_t, \\ l_{t+1} = b(\beta l_t - c_t^\lambda), \end{cases} \quad t \in \mathbb{Z}_+, \quad (33)$$

it is possible to define all two equilibria analytically:

$$E_1 = (0, 0), \quad E_2 = \left(\frac{1}{2} \left(\exp \left[\frac{\lambda \ln 2 + \ln \frac{\beta b - 1}{b}}{\lambda \gamma - 1} \right] \right)^\gamma, \exp \left[\frac{\lambda \ln 2 + \ln \frac{\beta b - 1}{b}}{\lambda \gamma - 1} \right] \right).$$

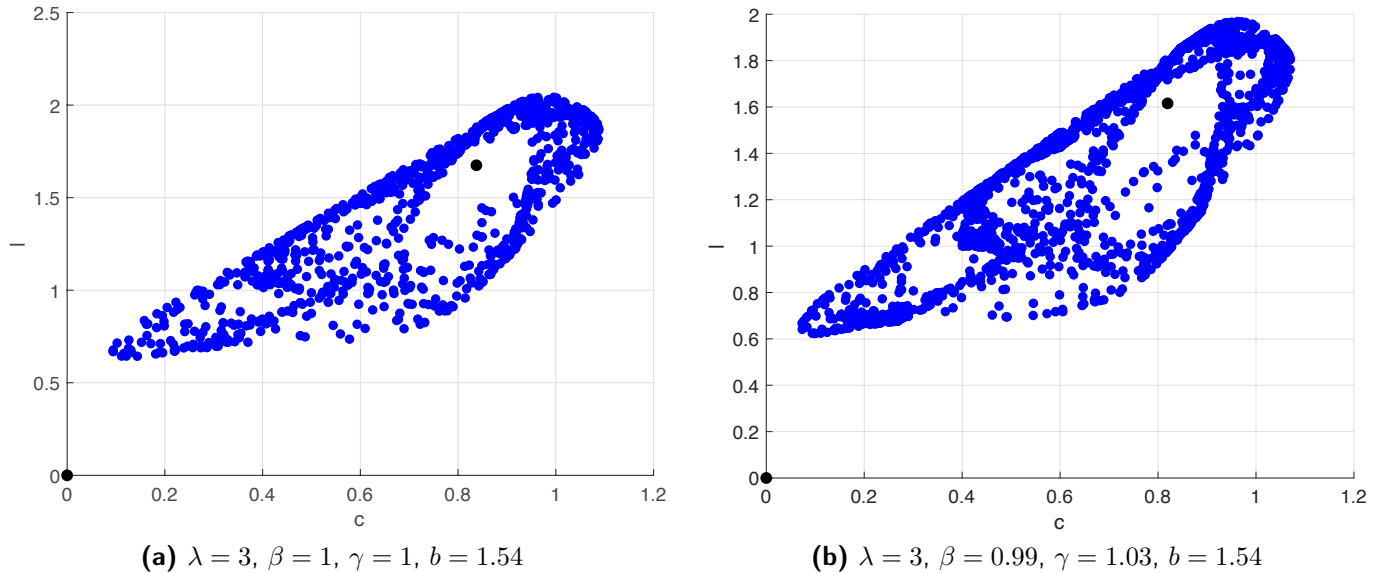


Figure 1: Chaotic attractors in OLG model (31) with parameters (34), (35).

In our work, for model (31) we study two groups of parameters for which this model has chaotic behavior. The first one,

$$\lambda = 3, \quad \beta = 1, \quad \gamma = 1, \quad b = 1.54, \quad (34)$$

does not satisfy conditions (32), but has only one nonlinearity with integer power, which makes the study of (31) much more simple.

The second one,

$$\lambda = 3, \quad \beta = 0.99, \quad \gamma = 1.03, \quad b = 1.54, \quad (35)$$

satisfies conditions (32), but provides more issues, because of noninteger power involved in the first equation.

3.2. Analysis of OLG model under control: searching for UPOs candidates

Dynamics of agent's consumption and labor in models (30) or (33) can be irregular with chaotic regime. Agents and controller (for instance, a government or decision-makers) strive to suppress this undesirable phenomenon. To solve this problem one can either stabilize an unstable equilibrium (which is rather simple task), or stabilize UPO embedded in a chaotic attractor. However, it could happen that for some *a priori* given initial conditions, the agents are not capable of reaching the stationary state or even approaching it. In such a situation they would attempt to move to a trajectory with a more predictable dynamics, using a minimal control. The latter task requires to determine whether the corresponding chaotic attractor contains any period- m UPO, i.e. whether for (29) or (31) there any solution for the corresponding equations:

$$(c_t, l_t) = \varphi^m(c_t, l_t), \quad \text{or} \quad (c_t, l_t) = \psi^m(c_t, l_t), \quad m = 1, 2, \dots \quad (36)$$

In order to find such control, we therefore assume that local attractor of the model is filled with periodic trajectories that are densely, and possibly uniformly, distributed in it. Then it is natural to find some periodic trajectories and under assumption of phase space mixing⁵. In our case,

⁴Further on we will use $c_t = c_t^t$ since there is only the superscript t in (27).

⁵A strict theoretical proof of mixing of trajectories and of ergodicity which involves constructing an ergodic measure is a complicated task beyond the scope of our study. Fundamental results obtained in this direction are presented, for example, in [101, 102].

we could confirm existence of mixing in a reproducible numerical experiment, to expect that the current agents' trajectory will over time enter neighborhood of the chosen periodic solution. Then one could "turn on" a minimal control intervention and switch the dynamics to this closest periodic trajectory. Similarly, a controller could use a control function (labor tax in our OLG model) to affect the expectations of agents and derive policy using calculations obtained with a mathematical model. In fact, the agents and the controller could act within paradigm of the same strategy and to solve similar tasks – forecasting and further control of dynamics aimed at selecting the periodic trajectory which corresponds to some feasible predictable solution. Here we face the following problem: since the right-hand sides of models (29) and (31) represent polynomials with noninteger powers, the search of periodic orbits, in general, can be made only numerically, and as period of a periodic orbit increases, the search becomes more difficult, and some point can't be performed even by using special functions for numerical solving of nonlinear equations (e.g. `NSolve[...]` in Wolfram Mathematica, `vpasolve(...)` in Matlab and `fsolve(...)` in Maple).

In our work, to overcome this difficulty, as well as to further determine parameters of time-delay feedback control (DFC) within Pyragas procedure, we refer to the EAs. Today, there is a relatively rich set of EAs, which are divided into different subgroups according to the internal principles of their principles or the philosophy-natural processes from which they were derived (see, e.g. [38]). The most well-known algorithms are, of course, genetic algorithms [103], [104], which represent classical EAs as well as DE [36], which is considered one of the most powerful EAs today [39]. Others are particle swarm [105] or SOMA [37], which belong to the class of swarm algorithms. For more details on these fascinating algorithms, we recommend reading the literature [40], [41].

We use three most powerful and commonly used optimization algorithms including DE and two versions of the SOMA as listed below:

- DE/rand/1/bin [106], with $NP = 50$, $Cr = 0.9$, $F = 0.7$, $MaxIter = 400$;
- SOMA All To One strategy (SOMA ATO) [107, 108], with $popsiz = 50$, $PathLength = 3.0$, $Step = 0.15$, $PRT = 0.33$, $MaxFEs = 20,000$;
- SOMA Team To Team Adaptive strategy (SOMA T3A) [109, 110], with $popsiz = 50$, $N_{jump} = 10$, $m = 10$, $n = 5$, $k = 10$, $MaxFEs = 20,000$, $PRT = 0.05 + 0.90(FEs/MaxFEs)$, and $Step = 0.2 + 0.05 \cos(4\pi FEs/MaxFEs)$.

In order to find the period- m UPO we define the following cost function

$$CF(c_t, l_t) = |(c_t, l_t) - \psi^m(c_t, l_t)|, \quad (37)$$

and for $m = 2, \dots, 6$ will try to find its minimum over the bounded region

$$(c_t, l_t) \in [0.2, 1.2] \times [0.5, 2],$$

where chaotic attractors, corresponding to parameters (34), (35), are located (see Fig. 1)

As a result of this experiments we have the following conclusions:

1. For OLG model (31) with parameters (34), (35) there are no periodic orbits with periods up to $m = 5$.
2. The application of EAs allows us to find two different UPOs for $m = 5$ (see Table 1 and Fig. 2) and also two UPOs for $m = 6$ (see Table 2).

In the next section, let us apply Pyragas time-delay feedback control to stabilize these UPOs and suppress chaos in system (31), as well as discuss the pros and cons of this approach and abilities of EA.

Table 1: Period-5 UPOs in the OLG model (31) with parameters (34), (35).

parameters	UPO #1		UPO #2	
	c_t	l_t	c_t	l_t
$\lambda = 3,$ $\beta = 1,$ $\gamma = 1,$ $b = 1.54$	0.9952568895406113	1.937721684767445	0.7712647366689733	1.7125896948743826
	0.9424647952268337	1.4659007926044583	0.9413249582054093	1.930857252566295
	0.5234359973776246	0.9682995881563105	0.9895322943608857	1.6890043947380275
	0.44486359077868604	1.2703242075158732	0.6994721003771418	1.1089231076735928
	0.825460616737187	1.8207175062777983	0.409451007296451	1.1807157439654243
$\lambda = 3,$ $\beta = 0.99,$ $\gamma = 1.03,$ $b = 1.54$	0.49786228048149456	0.9336025046020485	0.9738430606936463	1.6456210369735524
	0.433817924634687	1.2333289032631394	0.6965540321966559	1.086625515820712
	0.807294938247322	1.7546020061352825	0.392783070128333	1.1362119035892562
	0.9771534043359568	1.8648192605089056	0.7477900042112287	1.63894775026562
	0.9228564283533333	1.4062615940651981	0.9156305428565081	1.854778559891481

Table 2: Period-6 UPOs in the OLG model (31) with parameters (34), (35).

parameters	UPO #1		UPO #2	
	c_t	l_t	c_t	l_t
$\lambda = 3,$ $\beta = 1,$ $\gamma = 1,$ $b = 1.54$	0.953087122876765	1.9918473398169698	0.2617410777499068	0.70299137243586226
	1.038760216940205	1.7341736162104449	0.4412502946859554	1.054992264689458
	0.6954133992702398	0.9445246126546086	0.6137419700035027	1.4923832432875062
	0.2491112133843688	0.9366631654566522	0.8786412732840034	1.942247084462244
	0.6875519520722834	1.4186545006371223	1.0636058111782403	1.946447282891131
	0.7311025485648389	1.6841896714416038	0.8828414717128895	1.1445825494627964
$\lambda = 3,$ $\beta = 0.99,$ $\gamma = 1.03,$ $b = 1.54$	0.4273286812836567	1.0161364030089455	0.2360482546696026	0.9156617884384985
	0.58929581591653	1.429028575075392	0.6771964100935968	1.3757633891989363
	0.8551196850911698	1.8635444387760938	0.7117966011772947	1.619228199241378
	1.0435523163634506	1.8782149605648737	0.9310132570707518	1.9132975959437064
	0.8705169693966347	1.1134243718563632	1.0198912029882221	1.6742505107908452
	0.2465019913947314	0.6816233239954528	0.6804459848155441	0.9188249019130864

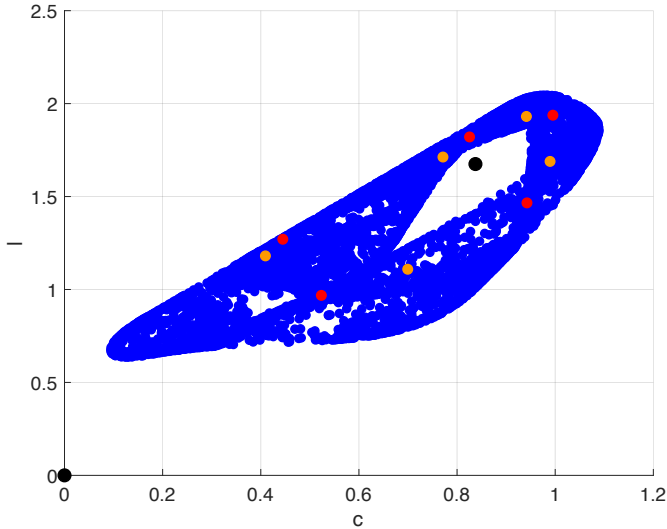
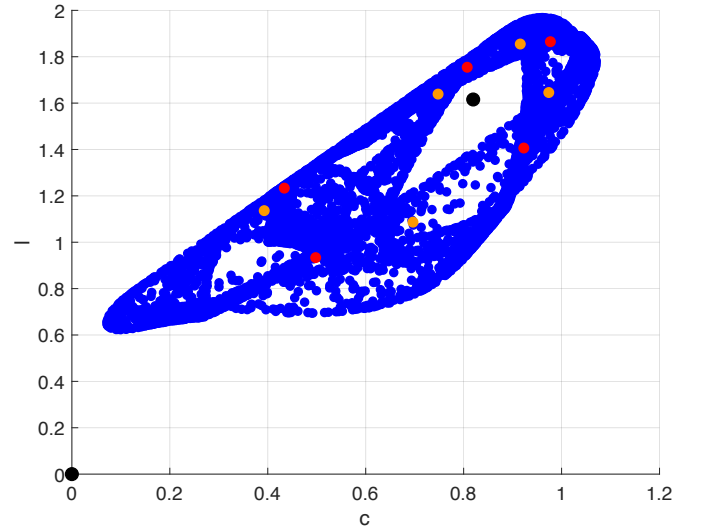

 (a) $\alpha = 3, \beta = 1, \gamma = 1, b = 1.54$

 (b) $\alpha = 3, \beta = 0.99, \gamma = 1.03, b = 1.54$

Figure 2: Period-5 UPOs (red, orange) embedded in the chaotic attractor (blue) in the OLG model (31) with parameters (34), (35).

3.3. Chaos suppression in the OLG model via DFC

In order to apply DFC to model (33), one needs to trace the values of the map at the previous iterations to form a time-delayed feedback control. This leads to the necessity of increasing the dimension of the initial map by the artificial addition of equations defining iterations at the previous steps. For instance, in order to stabilize the period- m UPO in model (33) one needs to store the previous iterations of the coordinates up to (c_{t-m}, l_{t-m}) . So, to apply DFC to this UPO by using additional control in the form (28) one needs to consider m additional equations (to store only one coordinate l_t) and the final system will have dimension $m + 2$; if one needs a control involving components $(c_t - c_{t-5})$ and $(l_t - l_{t-5})$, it will require consideration of $2m$ additional equations (to store both c_t and l_t variables), and the final system will have dimension $2m + 2$!

As we discussed above, control is introduced into the model through the variable g_t , which includes a proportional tax τ_t and labor l_t , which allows us to implement the control in a natural way. Consider OLG model (33)

$$\begin{cases} c_{t+1} = l_t^\gamma - c_t, \\ l_{t+1} = b(\beta l_t - c_t^\lambda - g_t), \end{cases} \quad t \in \mathbb{Z}_+,$$

with the DFC control in the form

$$g_t = k_1(l_t - l_{t-m}). \quad (38)$$

Consider the following extended 7d map assuming this form of control:

$$\begin{cases} c_{t+1} = l_t^\gamma - c_t, \\ l_{t+1} = b(\beta l_t - c_t^\alpha + k_1(l_t - l_t^{(5)})), \\ l_{t+1}^{(1)} = l_t + k_2(l_t - l_t^{(5)}), \\ l_{t+1}^{(2)} = l_t^{(1)} + k_3(c_t - c_t^{(5)}), \\ l_{t+1}^{(3)} = l_t^{(2)} + k_4(c_t - c_t^{(5)}), \\ l_{t+1}^{(4)} = l_t^{(3)} + k_5(c_t - c_t^{(5)}), \\ l_{t+1}^{(5)} = l_t^{(4)} + k_6(c_t - c_t^{(5)}). \end{cases} \quad (39)$$

The corresponding Jacobi matrix of (39) has the following form:

$$J(c_t, l_t) = \begin{pmatrix} -1 & \gamma l_t^{\gamma-1} & 0 & 0 & 0 & 0 & 0 \\ -\alpha b c_t^{\alpha-1} & b(\beta + k_1) & 0 & 0 & 0 & 0 & -b k_1 \\ 0 & 1 + k_2 & 0 & 0 & 0 & 0 & -k_2 \\ 0 & k_3 & 1 & 0 & 0 & 0 & -k_3 \\ 0 & k_4 & 0 & 1 & 0 & 0 & -k_4 \\ 0 & k_5 & 0 & 0 & 1 & 0 & -k_5 \\ 0 & k_6 & 0 & 0 & 0 & 1 & -k_6 \end{pmatrix}. \quad (40)$$

According to DFC, our aim is to find such k_1, \dots, k_6 for system (39) to make initially unstable period-5 periodic orbits from Table 1 locally orbitally stable. This is equivalent to have for the following fundamental matrix:

$$\Phi(c_t, l_t) = J(c_{t+4}, l_{t+4}) \cdot J(c_{t+3}, l_{t+3}) \cdot J(c_{t+2}, l_{t+2}) \cdot J(c_{t+1}, l_{t+1}) \cdot J(c_t, l_t) \quad (41)$$

calculated along the periodic orbits in Table (1) all absolute values of eigenvalues $\{|\lambda_i[\Phi]|\}_{i=1}^7$ less than unity. The latter is equivalent to have the spectral radius (i.e. the largest absolute value of eigenvalues) less than unity:

$$\rho[\Phi] = \max \{|\lambda_1[\Phi]|, \dots, |\lambda_7[\Phi]|\} < 1.$$

For simplicity, let us examine the controller with $k_3 = k_4 = k_5 = k_6 = 0$. In order to find k_1, k_2 we define the cost function

$$\text{CF}(k_1, k_2) = \rho[\Phi]^2. \quad (42)$$

The stabilization rate in the DFC depends on the stability of the periodic orbit (more stable periodic orbit \Rightarrow larger basin of attraction \Rightarrow faster stabilization), which in turn depends on how small it is possible to make absolute values for eigenvalues of fundamental matrix (41) by choosing the optimal values of the gain coefficients k_1, k_2 . In order to adjust the 'stability rate' of the periodic orbit it is also possible to experiment with the following cost functions, relying on the arithmetic mean $\bar{\lambda}[\Phi] = \frac{1}{7} \sum_{i=1}^7 |\lambda_i[\Phi]|$:

$$\text{CF}(k_1, k_2) = \begin{cases} \rho[\Phi]^2, & \rho[\Phi] \geq 1 \\ \text{CF}_{\text{temp}}(k_1, k_2), & \text{otherwise} \end{cases}, \quad \text{where} \quad \text{CF}_{\text{temp}}(k_1, k_2) = \bar{\lambda}[\Phi], \quad (43)$$

$$\text{CF}(k_1, k_2) = \begin{cases} \rho[\Phi]^2, & \rho[\Phi] \geq 1 \\ \text{CF}_{\text{temp}}(k_1, k_2), & \text{otherwise} \end{cases}, \quad \text{where} \quad \text{CF}_{\text{temp}}(k_1, k_2) = \sqrt{\frac{1}{7} \sum_{i=1}^7 (|\lambda_i[\Phi]| - \bar{\lambda}[\Phi])^2}. \quad (44)$$

Using EAs we try to find minimum of (42), (43), (44) over the region

$$(k_1, k_2) \in (-1, 1) \times (-1, 1).$$

As a result of this experiments we have the following conclusions:

1. Using DFC with the 'economical' control (38) it is possible to stabilize period-5 UPO#1 (see Table 1) for OLG model (33) with parameters (34), (35). All types of cost functions (42), (43), (44) here works.

Table 3: Parameters (k_1, k_2) for stabilization of UPO#1 (see Table 1) by DFC with the 'economical' control (38) in the OLG model (31) with parameters (34), (35).

paremeters	UPO #1		k_1	k_2
	c_t	l_t		
$\lambda = 3, \beta = 1,$ $\gamma = 1, b = 1.54$	0.9952568895406113	1.937721684767445	-0.13183153 -0.11874515	-0.88097316 -0.80453919
	0.9424647952268337	1.4659007926044583		
	0.5234359973776246	0.9682995881563105		
	0.44486359077868604	1.2703242075158732		
	0.825460616737187	1.8207175062777983		
$\lambda = 3,$ $\beta = 0.99,$ $\gamma = 1.03,$ $b = 1.54$	0.49786228048149456	0.9336025046020485	-0.18808852 -0.13998896 -0.19513422 -0.14491652	-0.95598289 -0.88037581 -0.97834281 -0.94132827
	0.433817924634687	1.2333289032631394		
	0.807294938247322	1.7546020061352825		
	0.9771534043359568	1.8648192605089056		
	0.9228564283533333	1.4062615940651981		

2. Using DFC with the 'economical' control (38) we are not able to stabilize UPO#2 (see Table 1) for OLG model (31) with parameters (34), (35). All cost functions (42), (43), (44) here does not work.

4. Optimal control problem to maximize the basin of attraction of stabilized UPO via DFC and EA

For given parameters of the model we can discover a periodic trajectory of the model and can show numerically that all solutions with initial conditions on a selected grid of points are always attracted to this periodic trajectory. However, implementation of numerical algorithms is complicated by numerical errors and the phenomenon of shadowing [111]. Imagine that within this economic model the agents possess perfect foresight and target a true periodic trajectory, while the controller receives information from the mathematical model by running a numerical experiment and selects a pseudo-trajectory in a neighborhood of this periodic trajectory. In this case an informational disbalance between the agents' and the controller's actions is possible, because it becomes difficult to guess when the forecasted periodic trajectory gets sufficiently close and whether this is the true or the pseudo-trajectory. It is therefore obvious that "turning on" of the control function in order to move to the periodic orbit is a complicated problem. Control could fail and attraction to the target trajectory will not happen. Of course, one could start the numerical process again and obtain another realization, attempting to achieve successful control intervention. This, however, does not preclude global errors while making a control decision. Therefore, we could postulate a following problem. Using EA and Pyragas control methods, optimize control parameters in such a way that the basin of attraction is maximized. Then, even if the current dynamics is far from the target periodic trajectory, the control will work in a more flexible regime, and attraction to the target solution will nevertheless occur. This will allow to reduce probability of the control failing to stabilize the dynamics, and thus to reduce potentially catastrophic losses of the agents' welfare.

In addition, using the Pyragas method allow to solve another important problem. Limited chaotic dynamics of the OLG model could also be observed when the model variables are outside of the feasible region of variables: for example, system's attractor is partially associated with negative values of some variables while the periodic solution is fully in the positive quadrant. In this case it is possible to use control for suppressing the chaotic behavior, return from the irregular to regular dynamics, and correct the behavior of the model in such a way that all variable values are located in the feasible set.

In this section, we demonstrate the abilities of EAs to solve a more difficult control problem of maximization of basins of attraction for stabilized UPOs. For OLG model in form (31), this problem is complicated by the fact that this model is dichotomic and not dissipative in the sense of Levinson (see e.g. [69, 112]), thus, the well-known methods of Lyapunov functions cannot be used to estimate the basins of attraction.

Consider delayed map (39) with Pyragas control parameters $(k_1, k_2) \in (-1, 1) \times (-1, 1)$, and $k_3 = k_4 = k_5 = k_6 = 0$. To compute the basin of attraction of stabilized UPO, we specify a rectangular area

$$[c_{\min}, c_{\max}] \times [l_{\min}, l_{\max}], \quad \text{where} \quad c_{\min} = l_{\min} = 0, \quad c_{\max} = 2, \quad l_{\max} = 3$$

and corresponding partition step

$$c_{\text{step}} = l_{\text{step}} = \varepsilon$$

to generate a grid $\mathcal{B}_{\text{grid}}(\varepsilon)$ consisting of $|\mathcal{B}_{\text{grid}}(\varepsilon)| = (2/\varepsilon + 1) \times (3/\varepsilon + 1)$ test points. Here $|A|$ denotes the cardinality of a set A .

Grid points correspond to the first and second coordinates of initial point for the OLG map (39):

$$(c_0, l_0) \in \mathcal{B}_{\text{grid}}(\varepsilon).$$

Five more (auxiliary) coordinates of the initial point (which we had to introduce to be able to consider delayed map with lag = 5) are considered as zeros:

$$l_0^{(1)} = l_0^{(2)} = l_0^{(3)} = l_0^{(4)} = l_0^{(5)} = 0.$$

For each initial point $(c_0, l_0, 0, 0, 0, 0, 0)$ of map (39) (where $(c_0, l_0) \in \mathcal{B}_{\text{grid}}(\varepsilon)$) we will perform N_{iter} iterations to trace the trajectory and depending on where this trajectory is attracted to divide the set

$$\mathcal{B}_{\text{grid}}(\varepsilon) = \mathcal{B}_{\text{inf}}(\varepsilon, k_1, k_2) \cup \mathcal{B}_{\text{upo}}(\varepsilon, N_{\text{iter}}, k_1, k_2) \cup \mathcal{B}_{\text{other}}(\varepsilon, N_{\text{iter}}, k_1, k_2)$$

into 3 subsets of initial points leading to different types of behavior:

- **Set $\mathcal{B}_{\text{inf}}(\varepsilon, k_1, k_2)$:** points, from which system's trajectories go to infinity;
- **Set $\mathcal{B}_{\text{upo}}(\varepsilon, N_{\text{iter}}, k_1, k_2)$:** points, from which system's trajectories after N_{iter} iterations tend to the stabilized UPO;
- **Set $\mathcal{B}_{\text{other}}(\varepsilon, N_{\text{iter}}, k_1, k_2)$:** points, from which system's trajectories after N_{iter} iterations tend to some other attractors.

The aim of our study here is for fixed predefined ε and N_{iter} to solve the following:

Optimal control problem: to find such values of control parameters (k_1, k_2) to maximize the number of points (cardinality) $|\mathcal{B}_{\text{upo}}(\varepsilon, N_{\text{iter}}, k_1, k_2)|$ of the basin of attraction $\mathcal{B}_{\text{upo}}(\varepsilon, N_{\text{iter}}, k_1, k_2)$ of the stabilized UPO:

$$\underset{(k_1, k_2)}{\text{maximize}} \left| \mathcal{B}_{\text{upo}}(\varepsilon, N_{\text{iter}}, k_1, k_2) \right|$$

w.r.t the chosen partition steps $c_{\text{step}} = l_{\text{step}} = \varepsilon$ and grid points $\mathcal{B}_{\text{grid}}(\varepsilon)$.

To solve this optimization problem using EAs we can consider the following cost functions:

$$\begin{aligned} \text{CF}(k_1, k_2) &= \left| \mathcal{B}_{\text{upo}}(\varepsilon, N_{\text{iter}}, k_1, k_2) \right| \rightarrow \max \quad \text{or} \\ \text{CF}(k_1, k_2) &= \left| \mathcal{B}_{\text{grid}}(\varepsilon) \right| - \left| \mathcal{B}_{\text{upo}}(\varepsilon, N_{\text{iter}}, k_1, k_2) \right| \rightarrow \min. \end{aligned} \quad (45)$$

Solving such an optimization problem implies calculation and examination of the behavior for the number of trajectories of system (39) equal to $|\mathcal{B}_{\text{grid}}(\varepsilon)|$ at each iteration of the evolutionary algorithm. As ε decreasing (to consider more dense grid of points) and N_{iter} increasing (to reveal the limiting behavior more accurately and to cut-off long transient regimes), it becomes an extremely time and resource consuming computational procedure. In order to speed up this procedure, we implement it on two powerful HPCs at IT4Innovations National Supercomputing Center of the Czech Republic. We use Parallel Computing Toolbox in Matlab R2015b and R2018a 64-bit versions to implement on two powerful clusters of Barbora and Salomon at IT4Innovations National Supercomputing Center⁶ of the Czech Republic, as listed below:

- **Barbora Cluster [113]:** under Red Hat Enterprise Linux 7.x operating system within 4 compute nodes, 36 cores of 2x18-core Intel Cascade Lake 6240 processors 2.6 GHz, at least 192 GB of RAM for each node (144 workers);
- **Salomon Cluster [114]:** under CentOS 7.x Linux operating system within 20 compute nodes, 2x Intel Xeon E5-2680v3, 2.5 GHz, 2x12 cores for each node (480 workers), and 5.3 GB per core, DDR4@2133 MHz.

Table 4: For procedure parameters $\varepsilon = 0.01$, $N_{\text{iter}} = 10000$, optimal parameters (k_1, k_2) for stabilization of UPO#1 by DFC with maximal basin of attraction for the OLG model (31) with parameters (34).

HPC	Evolutionary algorithm	Best member		$ \mathcal{B}_{\text{upo}}(\varepsilon, N_{\text{iter}}, k_1, k_2) $
		k_1	k_2	
Barbora	DE/rand/1/bin	-0.149784522963517	-0.886566828622060	5299
	SOMA	-0.146630592831770	-0.873678217705145	5631
	SOMA T3A	-0.141036797787322	-0.856600665432177	4724
Salomon	DE/rand/1/bin	-0.124379557961065	-0.873896102347582	2180
	SOMA	-0.146540835618650	-0.879197230586984	5693
	SOMA T3A	-0.147295233453928	-0.871914877265756	5728

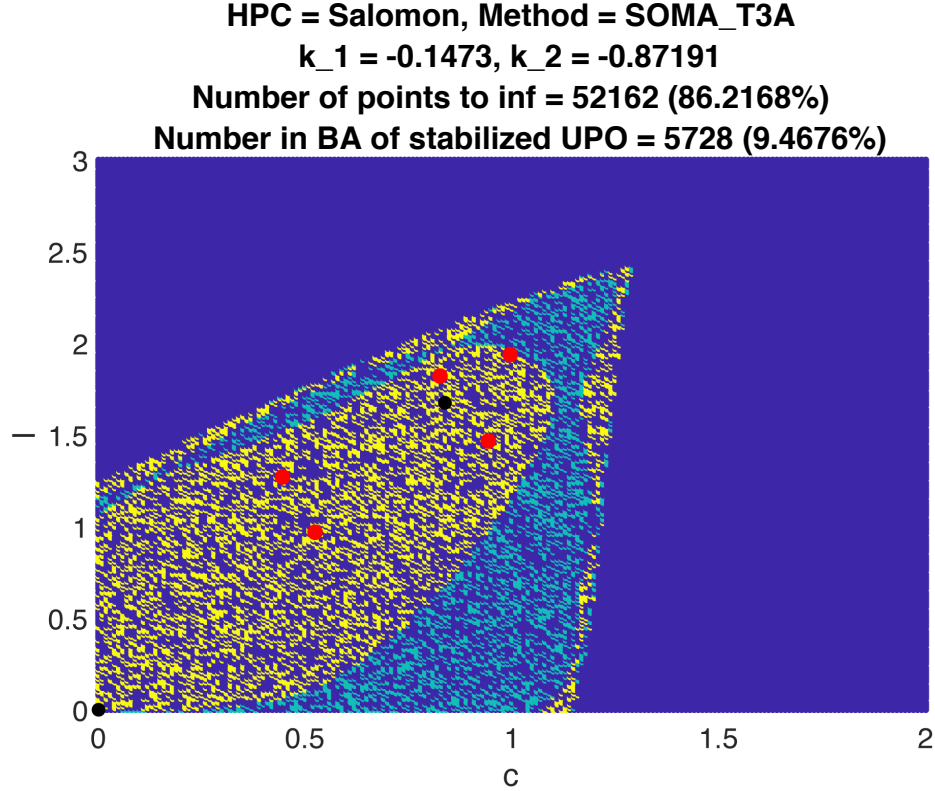


Figure 3: Basin of attraction (yellow) of stabilized UPO (red) with respect to optimal control parameters (k_1, k_2) for system (39) with parameters $\lambda = 3$, $\beta = 1$, $\gamma = 1$, $b = 1.54$. Purple domain corresponds to the points, from which trajectories go to infinity; cyan domain corresponds the points, from which trajectories go to other attractors.

In total 624 workers with 144 hours of calculation time at each run.

The results of maximal basin of attraction computation for stabilized UPO#1 (see Table 1 and Fig. 3) using three evolutionary algorithms (see Section 3.2) for system (39) with parameters $\lambda = 3$, $\beta = 1$, $\gamma = 1$, $b = 1.54$ and for procedure parameters $\varepsilon = 0.01$, $N_{\text{iter}} = 10000$ are presented in Table 4. The best value (i.e. the maximum number of points in $|\mathcal{B}_{\text{upo}}(\varepsilon, N_{\text{iter}}, k_1, k_2)| = 5728$) gave SOMA T3A launched on Salomon Cluster; however, it's interesting that SOMA T3A launched on Barbora Cluster gave one of the worst results (i.e. $|\mathcal{B}_{\text{upo}}(\varepsilon, N_{\text{iter}}, k_1, k_2)| = 4724$).

The overall simulation consumed about 344,714.12 core hours for the computation, equivalent to more than 39.35 continuously working years of the single CPU at 2.5 GHz.

⁶<https://www.it4i.cz/>

5. Conclusion

In this paper, we studied the properties of dynamics identifying regular and irregular modes, including chaotic ones in a discrete-time OLG model to improve forecasting its behavior. We constructed the OLG model with a control function. For the resulting model, we showed that in the absence of control, both regular and irregular behavior (periodic and chaotic) can be observed in it. Irregular behavior does not allow forecasting the limiting dynamics of the model, and therefore, decision-makers do not have the ability to predict and regulate the expectations of agents. The limiting chaotic dynamics of the OLG model can be observed when the range of admissible values of the model variables is violated.

To reveal the chaotic regime of the model's functioning, we used EA and found periodic trajectories embedded into the attractor. We applied the effective approach based on AI technologies and methods for stabilizing unstable dynamics for suppressing chaos to move from irregular to regular dynamics in the model, to correct behavior of the model, returning the values of variables to the admissible set by using small adjustments to the model parameters. To refine the found periodic trajectories, we used the Pyragas method, then we synthesized a control with two nonzero control parameters and select these parameters using the EA in such a way that the periodic trajectory becomes stable. Moreover, we selected the controls in such a way that the basin of attraction to the stable limiting dynamics is maximized. The combination of EAs with the Pyragas method significantly increased the efficiency of chaotic behavior control and allowed us much faster and fine-tuning of the control parameters to achieve the desired state of the model and the improvement of its forecasting behavior.

Acknowledgment

The following grants are acknowledged for the financial support provided for this research: St.Petersburg State University grant (Pure ID 75207094) [section 1], Leading Scientific Schools of Russia (project NSh-4196.2022.1.1) [section 2], the Russian Science Foundation project 22-11-00172 [section 4], the Ministry of Education, Youth and Sports of the Czech Republic through the e-INFRA CZ (ID:90140), Grant of SGS No. SP2022/22, VŠB-Technical University of Ostrava, Czech Republic.

References

- [1] R. Z. Aliber, C. P. Kindleberge, Manias, Panics, and Crashes: A History of Financial Crises, Palgrave Macmillan UK, 2015.
- [2] M. Scheffer, et al., Anticipating critical transitions, *Science* 338 (2012) 344–348.
- [3] S. Battiston, et.al., Complexity theory and financial regulationeconomic policy needs interdisciplinary network analysis and behavioral modeling, *Science* 351 (6275) (2016) 818–819.
- [4] J. Duffy, P. McNeli, Approximating and simulating the stochastic growth model: Parameterized expectations, neural networks, and the genetic algorithm, *Journal of Economic Dynamics and Control* 25 (9) (2001) 1273–1303.
- [5] L. Einav, J. Levin, Economics in the age of big data, *Science* 346 (6210) (2014) 1243089.
- [6] M. Jordan, T. Mitchell, Machine learning: Trends, perspectives, and prospects, *Science* 349 (6245) (2015) 255–260.
- [7] I. Goodfellow, Y. Bengio, A. Courville, *Deep Learning*, MIT Press, 2016.

- [8] M. Sendhil, J. Spiess, Machine learning: An applied econometric approach, *Journal of Economic Perspectives* 31 (2) (2017) 87–106.
- [9] P. Aghion, B. Jones, C. Jones, Artificial Intelligence and Economic Growth, Chicago: University of Chicago Press, 2019, Ch. In: *The Economics of Artificial Intelligence: An Agenda*, pp. 237–290.
- [10] A. Agrawal, J. Gans, A. Goldfarb (Eds.), *The Economics of Artificial Intelligence*, National Bureau of Economic Research Conference Report University of Chicago Press, 2019.
- [11] V. Duarte, Machine learning for continuous-time economics, Social Science Research Network (2018).
- [12] S. Consoli, D. Reforgiato Recupero, M. Saisana (Eds.), *Data Science for Economics and Finance: Methodologies and Applications*, Springer, 2021.
- [13] L. Maliar, S. Maliar, P. Winant, Will artificial intelligence replace computational economists any time soon?, *CEPR Discussion Pape (DP14024)* (2019).
- [14] J. Fernández-Villaverde, G. Nuño, G. Sorg-Langhans, M. Vogler, Solving high-dimensional dynamic programming problems using deep learning, National Bureau of Economic Research (2020).
- [15] P. Beaudry, D. Galizia, F. Portier, Putting the cycle back into business cycle analysis, *American Economic Review* 110 (1) (2020) 1–47.
- [16] Y. LeCun, Y. Bengio, G. Hinton, Deep learning, *Nature* 521 (7553) (2015) 436–444.
- [17] J. Sanders, J. Farmer, T. Galla, The prevalence of chaotic dynamics in games with many players, *Scientific Reports* 8 (2018) 4902.
- [18] N. Bloom, Fluctuations in uncertainty, *Journal of Economic Perspectives* 28 (2) (2014) 153–176.
- [19] S. R. Baker, N. Bloom, S. J. Davis, Measuring economic policy uncertainty, *The Quarterly Journal of Economics* 131 (4) (2016) 1593–1636.
- [20] S. Hansen, M. McMahon, Shocking language: Understanding the macroeconomic effects of central bank communication, *Journal of International Economics* 99 (2016) S114–S133.
- [21] S. Casella, J. Fernández-Villaverde, S. Hansen, Structural estimation of dynamic equilibrium models with unstructured data, *Mimeo*, University of Pennsylvania (2020).
- [22] D. Giannone, L. Reichlin, D. Small, Nowcasting: The real-time informational content of macroeconomic data, *Journal of Monetary Economics* 55 (4) (2008) 665–676.
- [23] V. Marx, The big challenges of big data, *Nature* 498 (2013) 255–260.
- [24] L. Barbaglia, S. Consoli, S. Manzan, Monitoring the business cycle with fine-grained, aspect-based sentiment extraction from news, in: V. Bitetta, I. Bordino, A. Ferretti, F. Gullo, S. Pascolutti, G. Ponti (Eds.), *Mining Data for Financial Applications*, Springer International Publishing, 2020, pp. 101–106.

- [25] S. Consoli, L. T. Pezzoli, E. Tosetti, Using the GDELT dataset to analyse the Italian sovereign bond market, in: G. Nicosia, V. Ojha, E. La Malfa, G. Jansen, V. Sciacca, P. Pardalos, G. Giuffrida, R. Umeton (Eds.), *Machine Learning, Optimization, and Data Science*, Springer International Publishing, 2020, pp. 190–202.
- [26] P. C. Tetlock, Giving content to investor sentiment: The role of media in the stock market, *Journal of Finance* 62 (3) (2007) 1139–1168.
- [27] A. Calvó-Armengol, Y. Zenou, Job matching, social network and word-of-mouth communication, *Journal of Urban Economics* 57 (3) (2005) 500–522.
- [28] A. Calvó-Armengoi, Y. Zenou, Social networks and crime decisions: The role of social structure in facilitating delinquent behavior, *International Economic Review* 45 (3) (2004) 939–958.
- [29] P. M. R. S. Cetina, Jill, Stressed to the core: Counterparty concentrations and systemic losses in cds markets, *Journal of Financial Stability* 35 (C) (2018) 38–52.
- [30] J. Boivin, M. Giannoni, DSGE models in a data-rich environment, *National Bureau of Economic Research* (w12772) (2006).
- [31] J. Fernández-Villaverde, S. Hurtado, G. Nuño, Financial frictions and the wealth distribution, *National Bureau of Economic Research* (w26302) (2019).
- [32] J. Fernández-Villaverde, P. A. Guerrón-Quintana, Estimating DSGE models: Recent advances and future challenges, *National Bureau of Economic Research* (w27715) (2020).
- [33] M. Azinovic, L. Gaegauf, S. Scheidegger, Deep equilibrium nets, *Social Science Research Network* (2019).
- [34] S. Kudyba, T. Davenport, Machine learning can help b2b firms learn more about their customers, *Harvard business review* (Jan. 2018).
- [35] D. Parkes, M. Wellman, Economic reasoning and artificial intelligence, *Science* 349 (6245) (2015) 267–272.
- [36] K. V. Price, Differential evolution, in: *Handbook of optimization*, Springer, 2013, pp. 187–214.
- [37] D. Davendra, I. Zelinka, et al., Self-organizing migrating algorithm, *New optimization techniques in engineering* (2016).
- [38] I. Zelinka, Real-time deterministic chaos control by means of selected evolutionary techniques, *Engineering Applications of Artificial Intelligence* 22 (2) (2009) 283–297.
- [39] Bilal, M. Pant, H. Zaheer, L. Garcia-Hernandez, A. Abraham, Differential evolution: A review of more than two decades of research, *Engineering Applications of Artificial Intelligence* 90 (2020) 103479.
- [40] D. Dasgupta, Z. Michalewicz, *Evolutionary algorithms in engineering applications*, Springer Science & Business Media, 2013.
- [41] T. Bäck, H.-P. Schwefel, An overview of evolutionary algorithms for parameter optimization, *Evolutionary computation* 1 (1) (1993) 1–23.

- [42] J.-M. Grandmont, On endogenous competitive business cycles, *Econometrica* 53 (5) (1985) 995–1045.
- [43] K. Adam, Learning and equilibrium selection in a monetary Overlapping Generations model with sticky prices, *The Review of Economic Studies* 70 (4) (2003) 887–907.
- [44] J. Benhabib, R. Day, Rational choice and erratic behaviour, *Review of Economic Studies* XLVIII (1981) 459–471.
- [45] R. H. Day, The emergence of chaos from classical economic growth, *The Quarterly Journal of Economics* 98 (2) (1983) 201–213.
- [46] W. Barnett, P. Chen, Deterministic chaotic and fractal attractors as tools for nonparametric dynamical econometric inference: With an applications to divisia monetary aggregates, *Mathematical Computational Modelling* 10 (1988) 275–296.
- [47] A. Medio, *Chaotic Dynamics: Theory and Applications to Economics*, Cambridge University Press, 1992.
- [48] C. Hommes, A reconsideration of Hicks’ non-linear trade cycle model, *Structural change and economic dynamics* 6 (1995) 435–459.
- [49] W. A. Brock, C. H. Hommes, A rational route to randomness, *Econometrica* 65, 1059–1095 (1997). 65 (1997) 1059–1095.
- [50] M. Kopel, Improving the performance of an economic system: controlling chaos, *Journal of Evolutionary Economics* 7 (1997) 269–289.
- [51] W. Brock, C. L. Sayers, Is the business cycle characterized by deterministic chaos?, *Journal of Monetary Economics* 22 (1998) 71–90.
- [52] W. Barnett, A. Serletis, Martingales, nonlinearity, and chaos, *Journal of Economic Dynamics and Control* 24 (2000) 703–724.
- [53] J. Rosser, *From catastrophe to chaos: A general theory of economic discontinuities*, Vol. 1. Mathematics, Microeconomics, Macroeconomics, and Finance, Springer Netherlands, 2000.
- [54] J. Benhabib, S. Schmitt-Grohe, M. Uribe, Chaotic interest rate rules, *American Economic Review* 92 (2002) 72–78.
- [55] C. Wieland, F. Westerhoff, Exchange rate dynamics, central bank interventions and chaos control methods, *Journal of Economic Behavior & Organization* 4 (2) (2005) 189–194.
- [56] C. Hommes, *Handbook of Computational Economics*, Vol. 2, Elsevier, 2006, Ch. 23, pp. 1109–1186.
- [57] R. Neck, Control theory and economic policy: Balance and perspectives, *Annual Reviews in Control* 33 (2009) 79–88.
- [58] H. Salarieh, A. Alasty, Chaos control in an economic model via minimum entropy strategy, *Chaos, Solitons & Fractals* 40 (2009) 839–847.
- [59] R. Amrit, J. Rawlings, D. Angeli, Economic optimization using model predictive control with a terminal cost, *Annual Reviews in Control* 35 (2011) 178–186.

- [60] F. Cavalli, A. Naimzada, N. Pecora, Real and financial market interactions in a multiplier-accelerator model: Nonlinear dynamics, multistability and stylized facts, *Chaos* 27 (2017) 103–120.
- [61] G. Bella, Homoclinic bifurcation and the Belyakov degeneracy in a variant of the Romer model of endogenous growth, *Chaos, Solitons & Fractals* 104 (2017) 452–460.
- [62] G. Bella, P. Mattana, B. Venturi, Shilnikov chaos in the Lucas model of endogenous growth, *Journal of Economic Theory* 172(C) (2017) 451–477.
- [63] T. Alexeeva, T. Mokaev, I. Polshchikova, Dynamics of monetary and fiscal policy in a New Keynesian model in continuous time, *Differentsialnye Uravnenia i Protsesy Upravleniya/Differential Equations and Control Processes* (4) (2020) 88–114.
- [64] T. Alexeeva, N. Kuznetsov, T. Mokaev, I. Polshchikova, Optimal control in the New Keynesian model with monetary and fiscal policy interactions, *Journal of Physics: Conference Series* 1864 (2021) 012040.
- [65] W. Barnett, G. Bella, T. Ghosh, P. Mattana, B. Venturi, Shilnikov chaos, low interest rates, and New Keynesian macroeconomics., *Working paper series in theoretical and applied economics* (2020).
- [66] D. Galizia, Saddle cycles: Solving rational expectations models featuring limit cycles (or chaos) using perturbation methods, *Quantitative Economics* 12 (3) (2021) 869–901.
- [67] G. Leonov, N. Kuznetsov, Hidden attractors in dynamical systems. From hidden oscillations in Hilbert-Kolmogorov, Aizerman, and Kalman problems to hidden chaotic attractors in Chua circuits, *International Journal of Bifurcation and Chaos in Applied Sciences and Engineering* 23 (1), art. no. 1330002 (2013). [doi:10.1142/S0218127413300024](https://doi.org/10.1142/S0218127413300024).
- [68] N. Kuznetsov, G. Leonov, Hidden attractors in dynamical systems: systems with no equilibria, multistability and coexisting attractors, *IFAC Proceedings Volumes* 47 (2014) 5445–5454, (survey lecture, 19th IFAC World Congress). [doi:10.3182/20140824-6-ZA-1003.02501](https://doi.org/10.3182/20140824-6-ZA-1003.02501).
- [69] G. Leonov, N. Kuznetsov, T. Mokaev, Homoclinic orbits, and self-excited and hidden attractors in a Lorenz-like system describing convective fluid motion, *The European Physical Journal Special Topics* 224 (8) (2015) 1421–1458. [doi:10.1140/epjst/e2015-02470-3](https://doi.org/10.1140/epjst/e2015-02470-3).
- [70] N. Kuznetsov, Hidden attractors in fundamental problems and engineering models. A short survey, *Lecture Notes in Electrical Engineering* 371 (2016) 13–25, (Plenary lecture at International Conference on Advanced Engineering Theory and Applications 2015). [doi:10.1007/978-3-319-27247-4_2](https://doi.org/10.1007/978-3-319-27247-4_2).
- [71] N. Kuznetsov, T. Mokaev, O. Kuznetsova, E. Kudryashova, The Lorenz system: hidden boundary of practical stability and the Lyapunov dimension, *Nonlinear Dynamics* 102 (2020) 713–732. [doi:10.1007/s11071-020-05856-4](https://doi.org/10.1007/s11071-020-05856-4).
- [72] T. A. Alexeeva, W. A. Barnett, N. V. Kuznetsov, T. N. Mokaev, Time-delay control for stabilization of the Shapovalov mid-size firm model, *IFAC-PapersOnLine* 53 (2) (2020) 16971–16976.
- [73] T. Alexeeva, N. Kuznetsov, T. Mokaev, Study of irregular dynamics in an economic model: attractor localization and Lyapunov exponents, *Chaos, Solitons & Fractals* 152 (2021) 111365.

- [74] K. Pyragas, Continuous control of chaos by self-controlling feedback, *Physics letters A* 170 (6) (1992) 421–428.
- [75] K. Pyragas, Delayed feedback control of chaos, *Phil. Trans. Royal Soc. A.* 369 (2006) 2039–2334.
- [76] P. Samuelson, An exact consumption-loan model of interest with or without the social contrivance of money, *Journal of Political Economy* 66 (6) (1958) 467–482.
- [77] P. Diamond, National debt in a neoclassical growth model, *American Economic Review* 55 (5) (1965) 1126–1150.
- [78] K. Farmer, R. Wendner, A two-sector Overlapping Generations model with heterogeneous capital, *Economic Theory* 22 (4) (2003) 773–792.
- [79] J. Benhabib, R. H. Day, A characterization of erratic dynamics in the Overlapping Generations model, *Journal of Economic Dynamics and Control* 4 (1982) 37–55.
- [80] W. Barnett, J. Geweke, K. Shell (Eds.), *Economic Complexity: Chaos, Sunspots, Bubbles, and Nonlinearity*, Cambridge University Press, 1989.
- [81] P. B. Dixon, W. Jorgensen, Dale (Eds.), *Handbook of Computable General Equilibrium Modeling*, North Holland, 2013.
- [82] G. Evans, S. Honkapohja, *Learning and Expectations in Macroeconomics*, Princeton University Press, 2001.
- [83] O. Galor, A two-sector Overlapping-Generations model: A global characterization of the dynamical system, *Econometrica* 60 (6) (1992) 1351–1386.
- [84] J. Arifovic, Genetic algorithms and inflationary economies, *Journal of Monetary Economics* (36) (1995) 219–243.
- [85] M. Woodford, Indeterminacy of equilibrium in the Overlapping Generations model: A survey, *Columbia Univ. mimeo* (1984).
- [86] P. Weil, Overlapping generations: The first jubilee, *Journal of Economic Perspectives* 22 (4) (2008) 115–134.
- [87] H. Fehr, S. Jokisch, M. Kallweit, F. Kindermann, L. J. Kotlikoff, Chapter 27 - generational policy and aging in closed and open dynamic general equilibrium models, in: P. B. Dixon, D. W. Jorgenson (Eds.), *Handbook of Computable General Equilibrium Modeling SET*, Vols. 1A and 1B, Vol. 1 of *Handbook of Computable General Equilibrium Modeling*, Elsevier, 2013, Ch. 27, pp. 1719–1800.
- [88] S. Nishiyama, K. Smetters, Analyzing Fiscal Policies in a Heterogeneous-Agent Overlapping-Generations Economy, Vol. 3, Elsevier, 2014, Ch. Chapter 3. *Handbook of Computational Economics*, pp. 117–160.
- [89] G. R. Zodrow, J. W. Diamond, Chapter 11 - dynamic overlapping generations computable general equilibrium models and the analysis of tax policy: The diamond–zodrow model, in: P. B. Dixon, D. W. Jorgenson (Eds.), *Handbook of Computable General Equilibrium Modeling SET*, Vols. 1A and 1B, Vol. 1 of *Handbook of Computable General Equilibrium Modeling*, Elsevier, 2013, Ch. 11.

- [90] M. Kurz, Chapter 8 - rational diverse beliefs and market volatility, in: T. Hens, K. R. Schenk-Hoppé (Eds.), *Handbook of Financial Markets: Dynamics and Evolution*, Handbooks in Finance, North-Holland, 2009, Ch. 8, pp. 439–506.
- [91] V. Quadrini, J.-V. Ríos-Rull, Chapter 14 - inequality in macroeconomics, in: A. B. Atkinson, F. Bourguignon (Eds.), *Handbook of Income Distribution*, Vol. 2 of *Handbook of Income Distribution*, Elsevier, 2015, Ch. 14, pp. 1229–1302.
- [92] A. Woodland, Chapter 12 - taxation, pensions, and demographic change, in: J. Piggott, A. Woodland (Eds.), *Handbook of the Economics of Population Aging*, Vol. 1 of *Handbook of the Economics of Population Aging*, North-Holland, 2016, Ch. 12, pp. 713–780.
- [93] A. Peralta-Alva, M. S. Santos, Chapter 9 - analysis of numerical errors, in: K. Schmedders, K. L. Judd (Eds.), *Handbook of Computational Economics Vol. 3*, Vol. 3 of *Handbook of Computational Economics*, Elsevier, 2014, Ch. 9, pp. 517–556.
- [94] M. K. Brunnermeier, M. Oehmke, Chapter 18 - bubbles, financial crises, and systemic risk, in: G. M. Constantinides, M. Harris, R. M. Stulz (Eds.), *Handbook of the Economics of Finance*, Vol. 2 of *Handbook of the Economics of Finance*, Elsevier, 2013, Ch. 18, pp. 1221–1288.
- [95] J. Arifovic, C. Hommes, I. Salle, Learning to believe in simple equilibria in a complex OLG economy - evidence from the lab, *Journal of Economic Theory* 183 (2019) 106–182.
- [96] K. J. Arrow, Uncertainty and the welfare economics of medical care, *American Economic Review* (53) (1963) 941–973.
- [97] J. Benhabib, K. Nishimura, *Indeterminacy and Sunspots with Constant Returns*, Springer Berlin Heidelberg, 2012, pp. 311–346.
- [98] M. Woodford, Three questions about sunspot equilibria as an explanation of economic fluctuations, *The American Economic Review* 77 (2) (1987) 93–98.
- [99] S. Slobodyan, Indeterminacy, sunspots, and development traps, *Journal of Economic Dynamics and Control* 29 (1) (2005) 159–185, computing in economics and finance.
- [100] D. Mendes, V. Mendes, Control of chaotic dynamics in an olg economic model, *J. Phys.: Conf. Series* 23 (2005) 158–181.
- [101] J.-P. Eckmann, D. Ruelle, Ergodic theory of chaos and strange attractors, *Reviews of Modern Physics* 57 (3) (1985) 617–656.
- [102] M. Benedicks, L.-S. Young, Sinai-Bowen-Ruelle measures for certain Henon maps, *Inventiones Mathematicae* 112 (1) (1993) 541–576.
- [103] J. H. Holland, Genetic algorithms, *Scientific american* 267 (1) (1992) 66–73.
- [104] M. Mitchell, *An introduction to genetic algorithms*, MIT press, 1998.
- [105] R. Eberhart, J. Kennedy, Particle swarm optimization, in: *Proceedings of the IEEE international conference on neural networks*, Vol. 4, Citeseer, 1995, pp. 1942–1948.
- [106] R. Storn, K. Price, Differential evolution—a simple and efficient heuristic for global optimization over continuous spaces, *Journal of global optimization* 11 (4) (1997) 341–359.

- [107] I. Zelinka, SOMA—self-organizing migrating algorithm, in: New optimization techniques in engineering, Springer, 2004, pp. 167–217.
- [108] I. Zelinka, SOMA—self-organizing migrating algorithm, in: Self-Organizing Migrating Algorithm, Springer, 2016, pp. 3–49.
- [109] Q. B. Diep, Self-organizing migrating algorithm team to team adaptive–SOMA T3A, in: 2019 IEEE Congress on Evolutionary Computation (CEC), IEEE, 2019, pp. 1182–1187.
- [110] Q. B. Diep, I. Zelinka, S. Das, R. Senkerik, SOMA T3A for solving the 100-digit challenge, in: Swarm, Evolutionary, and Memetic Computing and Fuzzy and Neural Computing, Springer, 2019, pp. 155–165.
- [111] S. Y. Pilyugin, Shadowing in dynamical systems, Springer, 2006.
- [112] N. Levinson, A second order differential equation with singular solutions, Ann. Math. 50 (1949) 127–153.
- [113] Barbora cluster hardware overview, <https://docs.it4i.cz/barbora/hardware-overview/>.
- [114] Salomon cluster hardware overview, <https://docs.it4i.cz/salomon/hardware-overview/>.

Appendix A. Procedure implementing chaos suppression in the OLG model via DFC

```

1 % OLG map with delay
2 function out = olgMapD(x, alpha, beta, gamma, b, K)
3
4     out = zeros(7,1);
5
6     % Coordinates:
7     % x(1) = c_i; x(2) = l_i; x(3) = c_{i-1}; ... x(7) = l_{i-5};
8
9     out(1) = x(2)^gamma - x(1);
10    out(2) = b * ( beta * x(2) - x(1)^alpha + K(1) * (x(2) - x(7)));
11    out(3) = x(2) + K(2) * (x(2) - x(7));
12    out(4) = x(3);
13    out(5) = x(4);
14    out(6) = x(5);
15    out(7) = x(6);
16 end

1 clearvars; clc;
2
3 numMapIter = 10000;
4 totalIter = numMapIter;
5
6 % Parameters:
7 alpha = 3; beta = 1; gamma = 1; b = 1.54;
8
9 % Equilibria:
10 S1 = [0, 0];
11
12 l_eq = exp((alpha*log(2) + log((beta * b - 1)/b)) / (alpha*gamma - 1));
13 c_eq = 0.5 * l_eq^gamma;
14
15 S2 = [c_eq, l_eq];
16
17 olgUP0 = [.4448636000, 1.270324210; ...
18           .8254646766, 1.820723642; ...
19           .9952568454, 1.937723390; ...
20           .9424648241, 1.465901543; ...
21           .5234360180, .9682995990];
22
23 % alpha = 3; beta = 0.99; gamma = 1.03; b = 1.54;
24 % olgUP0 = [.49786228048149456, .9336025046020485; ...
25 %           .433817924634687, 1.233328903263139; ...
26 %           .807294938247322, 1.7546020061352825; ...
27 %           .9771534043359568, 1.8648192605089056; ...
28 %           .9228564283533333, 1.4062615940651981];
29
30 [olgUP0_period, ~] = size(olgUP0);
31
32 K_EA = [-0.13; -0.9];
33
34 currPoint = [0.0, 0.1, 0, 0, 0, 0, 0];
35
36 olgSolPyr = zeros(numMapIter, 7);
37
38 olgSolPyr(1,:) = currPoint;
39

```

```

40 numPeriodChunks = 2;
41
42 trajTail = zeros(numPeriodChunks * olgUP0_period, 2);
43
44 for iMapIter = 2 : numMapIter
45     olgSolPyr(iMapIter, :) = olgMapD( currPoint, alpha, beta, gamma, b, K_EA)';
46
47     currPoint = olgSolPyr(iMapIter, :);
48
49 %     currPoint = feval(olgMapD, currPoint);
50
51 % tends to infity
52 if currPoint(2) < 0 || abs(currPoint(1)) > 2
53     totalIter = iMapIter;
54     break;
55 end
56 end
57
58 % Plot
59 figure; hold on;
60 % Trajectory with Pyragas stabilization (last 1000 iterations):
61 scatter(olgSolPyr(1:end, 1), olgSolPyr(1:end,2), 'filled','MarkerEdgeColor',[0,
    ↪ 0.6, 0], 'MarkerFaceColor', [0, 0.6, 0]);
62 % scatter(olgSolPyr(numMapIter-4 : numMapIter,1), olgSolPyr(numMapIter-4 :
    ↪ numMapIter,2), 'filled','MarkerEdgeColor',[0, 0.6, 0], 'MarkerFaceColor',
    ↪ [0, 0.6, 0]);
63 % UPO
64 scatter(olgUP0(:, 1), olgUP0(:,2), 'filled', 'SizeData', 50, 'MarkerEdgeColor',
    ↪ 'red', 'MarkerFaceColor', 'red');
65 % Equilibria:
66 plot(S1(1), S1(2), '.', 'markersize', 20, 'Color', 'black');
67 plot(S2(1), S2(2), '.', 'markersize', 20, 'Color', 'black');
68
69 hold off; grid on; axis on;
70 xlabel('c');
71 ylabel('l');
72 set(gca, 'FontSize', 14);
73
74 figure; hold on;
75 % Trajectory with Pyragas stabilization:
76 scatter(1 : totalIter, olgSolPyr(1 : totalIter, 1), 'filled','MarkerEdgeColor'
    ↪ , [0, 0.6, 0], 'MarkerFaceColor', [0, 0.6, 0]);
77 hold off; grid on; axis on;
78 xlabel('t (iteration)');
79 ylabel('c');
80 set(gca, 'FontSize', 14);
81
82 figure; hold on;
83 % Trajectory with Pyragas stabilization:
84 scatter(1 : totalIter, olgSolPyr(1 : totalIter, 7), 'filled','MarkerEdgeColor'
    ↪ , [0, 0.6, 0], 'MarkerFaceColor', [0, 0.6, 0]);
85 % scatter(numMapIter-1000 : numMapIter, olgSolPyr(numMapIter-1000 : numMapIter,
    ↪ 2), 'filled','MarkerEdgeColor',[0, 0.6, 0], 'MarkerFaceColor', [0, 0.6,
    ↪ 0]);
86 hold off; grid on; axis on;
87 xlabel('t (iteration)');
88 ylabel('c');
89 set(gca, 'FontSize', 14);

```


Appendix B. Procedure of solving an optimal control problem to maximize the basin of attraction of stabilized UPO via DFC and EA

Appendix B.1. Procedure, implementing calculation of the cost function (45).

```

1 function costValue = dfcParamCostFun(k1, k2, alpha, beta, gamma, b, gridPoints,
    ↪ olgUP0, numMapIter, numPeriodicChunks, periodicTol, vicTols, iTol)
2     % Current parameters for Pyragas control
3     % K_EA = [k1; k2];
4     % Evaluation of the grid of points
5     %vectFlags = computeBA_parallel(@(x) olgMapD(x, alpha, beta, gamma, b, K_EA
    ↪ ), gridPoints, olgUP0, numMapIter, numPeriodicChunks, periodicTol,
    ↪ vicTols);
6     %%%%%%%%%%%%%%%%%%%%%%%%%%%%%%%%%%%%%%%%%%%%%%%%%%%%%%%%%%%%%%%%%%%%%%%%%
7     [numGridPoints, ~] = size(gridPoints);
8     [olgUP0_period, ~] = size(olgUP0);
9     numVicTols = length(vicTols);
10    % By default, set flags = -1, as if all trajectories tend to infty
11    vectFlags = -ones(numGridPoints, numVicTols);
12    global time_parfor
13    time_temp = toc;
14    parfor iPoint = 1 : numGridPoints % parfor here
15        currPoint = [gridPoints{iPoint}, 0, 0, 0, 0, 0];
16        isToInf = 0;
17        trajTail = zeros(numPeriodicChunks * olgUP0_period, 2);
18        %%%%%%%%%%%%%%%%%%%%%%%%%%%%%%%%%%%%%%%%%%%%%%%%%%%%%%%%%%%%%%%%%%%%%%%%%
19        out = zeros(7,1);
20        num_temp = numMapIter - numPeriodicChunks * olgUP0_period;
21        %%%%%%%%%%%%%%%%%%%%%%%%%%%%%%%%%%%%%%%%%%%%%%%%%%%%%%%%%%%%%%%%%%%%%%%%%
22        for iMapIter = 2 : numMapIter
23            % currPoint = feval(olgMapD, currPoint);
24            %%%%%%%%%%%%%%%%%%%%%%%%%%%%%%%%%%%%%%%%%%%%%%%%%%%%%%%%%%%%%%%%%%%%%%%%%
25            % x = currPoint;
26            % out = zeros(7,1);
27            % Coordinates:
28            out(1) = currPoint(2)^gamma - currPoint(1);
29            out(2) = b * (beta * currPoint(2) - currPoint(1)^alpha + k1 * (
    ↪ currPoint(2) - currPoint(7)));
30            out(3) = currPoint(2) + k2 * (currPoint(2) - currPoint(7));
31            out(4) = currPoint(3);
32            out(5) = currPoint(4);
33            out(6) = currPoint(5);
34            out(7) = currPoint(6);
35            currPoint = out;
36            %%%%%%%%%%%%%%%%%%%%%%%%%%%%%%%%%%%%%%%%%%%%%%%%%%%%%%%%%%%%%%%%%%%%%%%%%
37            % terminate evolution of trajectory if it tends to infty
38            if abs(currPoint(1)) > 2
39                isToInf = 1;
40                break;
41            end
42            % cut the transient process and get
43            % the "tail" of trajectory to compare with UPO
44            if iMapIter > num_temp
45                trajTail(iMapIter - num_temp, :) = currPoint(1:2);
46            end
47        end
48        % if trajectory is not tending to infty and (almost) periodic, then
49        % save results of comparison of trajectory and UPO
50        %%%%%%%%%%%%%%%%%%%%%%%%%%%%%%%%%%%%%%%%%%%%%%%%%%%%%%%%%%%%%%%%%%%%%%%%%

```

```

51 % checkIsPeriodicTol
52 trajPeriodicChunks_x = reshape(trajTail(:,1), olgUP0_period, []);
53 trajPeriodicChunks_y = reshape(trajTail(:,2), olgUP0_period, []);
54 diff_x = abs(trajPeriodicChunks_x(:, 1:end-1) - trajPeriodicChunks_x
    ↪ (:,2:end));
55 diff_y = abs(trajPeriodicChunks_y(:, 1:end-1) - trajPeriodicChunks_y
    ↪ (:,2:end));
56 isPeriodic = all(diff_x < periodicTol) && all(diff_y < periodicTol);
57 if ~isToInf && isPeriodic
58     %%%%%%%%%%%%%%%%%%%%%%%%%%%%%%%%%%%%%%%%%%%%%%%%%%%%%%%%%%%%%
59     %vectFlags(iPoint, :) = compareTrajUP0(trajTail(1+end-olgUP0_period
    ↪ :end, :), olgUP0, vicTols);
60     %numVicTols = length(vicTols);
61     vectFlags_temp2 = zeros(1, numVicTols);
62     traj_x = sort(trajTail(1+end-olgUP0_period:end, 1));
63     traj_y = sort(trajTail(1+end-olgUP0_period:end, 2));
64     UP0_x = sort(olgUP0(:,1));
65     UP0_y = sort(olgUP0(:,2));
66     for iVicTol = 1 : numVicTols
67         currVicTol = vicTols(iVicTol);
68         % 1 (true) - if tending (stabilizing) to the target UP0 (within
    ↪ tolerance);
69         % 0 (false) - if tending somewhere else, or not tending at all;
70         vectFlags_temp2(iVicTol) = ...
71             all(ismembertol(traj_x, UP0_x, currVicTol, 'ByRows', true))
    ↪ && ...
72             all(ismembertol(traj_y, UP0_y, currVicTol, 'ByRows', true))
    ↪ ;
73     end
74     vectFlags(iPoint, :) = vectFlags_temp2;
75 end
76 end
77 time_parfor = time_parfor + toc - time_temp;
78 %%%%%%%%%%%%%%%%%%%%%%%%%%%%%%%%%%%%%%%%%%%%%%%%%%%%%%%%%%%%%
79 % Number of points in the basin of attraction
80 numPointsBA = sum(vectFlags == 1);
81 %[numGridPoints, ~] = size(gridPoints);
82 costValue = (numGridPoints - numPointsBA(iTol));
83 end

```

Appendix B.2. Main scripts to run the procedure using DE/rand/1/bin.

```

1 clearvars; clc;
2 diary('Results/DiaryFile_DE_ran1bin_10k.txt');
3 disp('Method: DE rand1bin 10k')
4 disp('-----')
5 % Define bounds of the grid:
6 cMin = 0; cMax = 2;
7 lMin = 0; lMax = 3;
8 % Test values of partition step
9 % cStep = 1; lStep = 1;
10 % ''Real'' values of partition step
11 cStep = 0.01; lStep = 0.01;
12 % Generate grid of points
13 [C, L] = meshgrid(cMin:cStep:cMax, lMin:lStep:lMax);
14 vectC = C(:); vectL = L(:);
15 gridPoints = num2cell([C(:), L(:)], 2);
16 % Set parameters of OLG map (with chaos):

```

```

17 alpha = 3; beta = 1; gamma = 1; b = 1.54;
18 % Define corresponding UPO to stabilize:
19 olgUPO = [.4448636000, 1.270324210; ...
20           .8254646766, 1.820723642; ...
21           .9952568454, 1.937723390; ...
22           .9424648241, 1.465901543; ...
23           .5234360180, .9682995990];
24 % Set number of iterations of delayed OLG map:
25 numMapIter = 1e3*10;
26 % Length of trajectory's "tail" = number of chunks * period
27 numPeriodicChunks = 2;
28 % Tolerance to consider trajectory's "tail" being periodic
29 periodicTol = 1e-5;
30 % Set the size of vicinity of UPO to check stabilization:
31 vicTols = 1e-1;
32 iTol = 1;
33 %%%%%%%%%%%%%%%%%%%%%%%%%%%%%%%%%%%%%%%%%%%%%%%%%%%%%%%%%%%%%%%%%%%%%%%%%
34 % Define parameters for DE:
35 popsize = 50;
36 Max_Gen = 400; % <=> Max_FEs = 20000
37 Cr = 0.9; F = 0.7;
38 Xmin = -0.3; Xmax = 0;
39 Ymin = -1.0; Ymax = -0.7;
40 Dim = 2;
41 CostFunction = @(pop) arrayfun(@(k1, k2) dfcParamCostFun(k1, k2, alpha,...
42     beta, gamma,b , gridPoints, olgUPO, numMapIter, numPeriodicChunks,...
43     periodicTol, vicTols, iTol), pop(:,1), pop(:,2));
44 %%%%%%%%%%%%%%%%%%%%%%%%%%%%%%%%%%%%%%%%%%%%%%%%%%%%%%%%%%%%%%%%%%%%%%%%%
45 filetxt = 'Results/Results_DE_ran1bin_10k.txt';
46 filemat = 'Results/DFC_DE_ran1bin_10k_in.mat';
47 fileID = fopen(filetxt, 'a');
48 fprintf(fileID, 'FEs,best_cost,X,Y,time_flow,time_step,time_parfor\n');
49 fclose(fileID);
50 global time_parfor time_step
51 time_parfor = 0; time_step = 0;
52 tic
53 % ----- Create Initial Population -----
54 pop = Xmin + (Xmax-Xmin).*rand(popsize,1);
55 pop(:,2) = Ymin + (Ymax-Ymin).*rand(popsize,1);
56 fit = CostFunction(pop);
57 FEs = popsize;
58 [best_fit,id] = min(fit);
59 best_val = pop(id,:);
60 Store_and_Display(filetxt,FEs,best_fit,best_val);
61 for gen = 1 : Max_Gen-1
62     % Combined Steps: Mutation+Crossover+Selection...to generate new pop
63     FM_mui = rand(popsize,Dim) < Cr;
64     A1 = randperm(popsize);
65     A2 = circshift(A1,1);
66     A3 = circshift(A2,2);
67     newpop = pop(A1,:) + F*(pop(A2,:)-pop(A3,:));
68     newpop = pop.*not(FM_mui) + newpop.*FM_mui;
69     % Check the boundary and replace individuals
70     newpop(:,1) = max(newpop(:,1),Xmin);
71     newpop(:,1) = min(newpop(:,1),Xmax);
72     newpop(:,2) = max(newpop(:,2),Ymin);
73     newpop(:,2) = min(newpop(:,2),Ymax);
74     % Evaluate the new population
75     newfit = CostFunction(newpop);

```

```

76     FEs          = FEs + popsize;
77     % Update the new population
78     idx          = newfit <= fit;
79     fit(idx)     = newfit(idx);
80     pop(idx,:)   = newpop(idx,:);
81     % Update the Global Best
82     [min_fit,id] = min(newfit);
83     if min_fit < best_fit
84         best_fit = min_fit;
85         best_val = newpop(id,:);
86     end
87     %====Store and Display Results =====
88     try
89         Store_and_Display(filetxt,FEs,best_fit,best_val);
90         save(filemat)
91     catch
92         fprintf('Error while saving! Skipped this time. \n')
93     end
94 end % END Loop
95 disp('DONE!')
96 diary off
97 %%%%%%%%%%%%%%%%%%%%%%%%%%%%%%%%%%%%%%%%%%%%%%%%%%%%%%%%%%%%%%%%%%%%%%%%%

```

Appendix B.3. Main scripts to run the procedure using SOMA.

```

1  clearvars; clc;
2  diary('Results/DiaryFile_SOMA_Classic_10k.txt');
3  disp('Method: SOMA Classic 10k')
4  disp('-----')
5  % Define bounds of the grid:
6  cMin = 0; cMax = 2;
7  lMin = 0; lMax = 3;
8  % Test values of partition step
9  % cStep = 1; lStep = 1;
10 % ''Real'' values of partition step
11 cStep = 0.01; lStep = 0.01;
12 % Generate grid of points
13 [C, L] = meshgrid(cMin:cStep:cMax, lMin:lStep:lMax);
14 vectC = C(:); vectL = L(:);
15 gridPoints = num2cell([C(:), L(:)], 2);
16 % Set parameters of OLG map (with chaos):
17 alpha = 3; beta = 1; gamma = 1; b = 1.54;
18 % Define corresponding UPO to stabilize:
19 olgUPO = [.4448636000, 1.270324210; ...
20           .8254646766, 1.820723642; ...
21           .9952568454, 1.937723390; ...
22           .9424648241, 1.465901543; ...
23           .5234360180, .9682995990];
24 % Set number of iterations of delayed OLG map:
25 numMapIter = 1e3*10;
26 % Length of trajectory's "tail" = number of chunks * period
27 numPeriodicChunks = 2;
28 % Tolerance to consider trajectory's "tail" being periodic
29 periodicTol = 1e-5;
30 % Set the size of vicinity of UPO to check stabilization:
31 vicTols = 1e-1;
32 iTol = 1;
33 %%%%%%%%%%%%%%%%%%%%%%%%%%%%%%%%%%%%%%%%%%%%%%%%%%%%%%%%%%%%%%%%%%%%%%%%%

```

```

34 % ----- Initial Parameters of SOMA -----
35 Step      = 0.15;    % Define the Step parameter
36 PRT       = 0.33;    % Define the PRT parameter
37 popsize   = 50;      % Define the number individuals of the population
38 PathLen   = 3;       % Define the PathLength parameter
39 Max_FEs   = 20000;   % Define the stop condition
40 Xmin      = -0.3; Xmax = 0;
41 Ymin      = -1.0; Ymax = -0.7;
42 Dim       = 2;
43 CostFunction = @(pop) arrayfun(@(k1, k2) dfcParamCostFun(k1, k2, alpha,...
44     beta, gamma,b , gridPoints, olgUP0, numMapIter, numPeriodicChunks,...
45     periodicTol, vicTols, iTol), pop(:,1), pop(:,2));
46 %%%%%%%%%%%%%%%%%%%%%%%%%%%%%%%%%%%%%%%%%%%%%%%%%%%%%%%%%%%%%%%%%%%%%%%%%
47 filetxt = 'Results/Results_SOMA_Classic_10k.txt';
48 filemat = 'Results/DFC_SOMA_Classic_10k_in.mat';
49 fileID = fopen(filetxt, 'a');
50 fprintf(fileID, 'FEs,best_cost,X,Y,time_flow,time_step,time_parfor\n');
51 fclose(fileID);
52 global time_parfor time_step
53 time_parfor = 0; time_step = 0;
54 tic
55 % ----- Create Initial Population -----
56 pop      = Xmin + (Xmax-Xmin).*rand(popsize,1);
57 pop(:,2) = Ymin + (Ymax-Ymin).*rand(popsize,1);
58 fit      = CostFunction(pop);
59 FEs      = popsize;
60 [best_fit,id] = min(fit);
61 best_val    = pop(id,:);
62 Store_and_Display(filetxt,FEs,best_fit,best_val);
63 while FEs < Max_FEs
64     [~,idL] = min(fit);
65     leader  = pop(idL,:);
66     % ----- movement of each individual -----
67     for j = 1 : popsize
68         if j ~= idL
69             moving      = pop(j,:);
70             nstep       = (Step:Step:PathLen)';
71             PRTVector   = rand(length(nstep),Dim) < PRT;
72             newpop      = moving+(leader-moving).*nstep.*PRTVector;
73             %-- Check the boundary and replace the Individuals
74             newpop(:,1) = max(newpop(:,1),Xmin);
75             newpop(:,1) = min(newpop(:,1),Xmax);
76             newpop(:,2) = max(newpop(:,2),Ymin);
77             newpop(:,2) = min(newpop(:,2),Ymax);
78             %----- Evaluate the offspring -----
79             newfit      = CostFunction(newpop);
80             FEs         = FEs + length(nstep);
81             %----- Choose the best offspring -----
82             [min_fit,id] = min(newfit);
83             %----- Update the best value -----
84             if min_fit <= fit(j)
85                 pop(j,:) = newpop(id,:);
86                 fit(j)   = min_fit;
87                 if min_fit < best_fit
88                     best_fit = min_fit;
89                     best_val = newpop(id,:);
90                 end
91             end
92         %===Store and Display Results =====

```

```

93         try
94             Store_and_Display(filetxt,FEs,best_fit,best_val);
95             save(filemat)
96         catch
97             fprintf('Error while saving! Skipped this time. \n')
98         end
99         %-----
100     end % END if j ~= idL
101 end % for j = 1 : popSize
102 end % END Loop
103 disp('DONE!')
104 diary off
105 %%%%%%%%%%%%%%%%%%%%%%%%%%%%%%%%%%%%%%%%%%%%%%%%%%%%%%%%%%%%%%%%%%%%%%%%%

```

Appendix B.4. Main scripts to run the procedure using SOMA T3A.

```

1 clearvars; clc;
2 diary('Results/DiaryFile_SOMA_T3A_10k.txt');
3 disp('Method: SOMA T3A 10k')
4 disp('-----')
5 % Define bounds of the grid:
6 cMin = 0; cMax = 2;
7 lMin = 0; lMax = 3;
8 % Test values of partition step
9 % cStep = 1; lStep = 1;
10 % ''Real'' values of partition step
11 cStep = 0.01; lStep = 0.01;
12 % Generate grid of points
13 [C, L] = meshgrid(cMin:cStep:cMax, lMin:lStep:lMax);
14 vectC = C(:); vectL = L(:);
15 gridPoints = num2cell([C(:), L(:)], 2);
16 % Set parameters of OLG map (with chaos):
17 alpha = 3; beta = 1; gamma = 1; b = 1.54;
18 % Define corresponding UPO to stabilize:
19 olgUPO = [.4448636000, 1.270324210; ...
20           .8254646766, 1.820723642; ...
21           .9952568454, 1.937723390; ...
22           .9424648241, 1.465901543; ...
23           .5234360180, .9682995990];
24 % Set number of iterations of delayed OLG map:
25 numMapIter = 1e3*10;
26 % Length of trajectory's "tail" = number of chunks * period
27 numPeriodicChunks = 2;
28 % Tolerance to consider trajectory's "tail" being periodic
29 periodicTol = 1e-5;
30 % Set the size of vicinity of UPO to check stabilization:
31 vicTols = 1e-1;
32 iTol = 1;
33 %%%%%%%%%%%%%%%%%%%%%%%%%%%%%%%%%%%%%%%%%%%%%%%%%%%%%%%%%%%%%%%%%%%%%%%%%
34 % ----- Initial Parameters of SOMA -----
35 popsize = 50; % Define the number individuals of the population
36 N_jump = 10; % Define the PathLength parameter
37 Max_FEs = 20000; % Define the stop condition
38 m = 10; % The parameter m
39 n = 5; % The parameter n
40 k = 10; % The parameter k
41 Xmin = -0.3; Xmax = 0;
42 Ymin = -1.0; Ymax = -0.7;

```

```

43 Dim = 2;
44 CostFunction = @(pop) arrayfun(@(k1, k2) dfcParamCostFun(k1, k2, alpha,...
45     beta, gamma,b , gridPoints, olgUP0, numMapIter, numPeriodicChunks,...
46     periodicTol, vicTols, iTol), pop(:,1), pop(:,2));
47 %%%%%%%%%%%%%%%%%%%%%%%%%%%%%%%%%%%%%%%%%%%%%%%%%%%%%%%%%%%%%%%%%%%%%%%%%
48 filetxt = 'Results/Results_SOMA_T3A_10k.txt';
49 filemat = 'Results/DFC_SOMA_T3A_10k_in.mat';
50 fileID = fopen(filetxt, 'a');
51 fprintf(fileID, 'FES,best_cost,X,Y,time_flow,time_step,time_parfor\n');
52 fclose(fileID);
53 global time_parfor time_step
54 time_parfor = 0; time_step = 0;
55 tic
56 % ----- Create Initial Population -----
57 pop = Xmin + (Xmax-Xmin).*rand(popsize,1);
58 pop(:,2) = Ymin + (Ymax-Ymin).*rand(popsize,1);
59 fit = CostFunction(pop);
60 FEs = popsize;
61 [best_fit,id] = min(fit);
62 best_val = pop(id,:);
63 Store_and_Display(filetxt, FEs, best_fit, best_val);
64 while FEs+N_jump < Max_FEs
65     % ----- Migrant selection: m -----
66     M = randperm(popsize,m);
67     [~,Im] = mink(fit(M),n);
68     % ----- movement of each individual -----
69     for j = 1 : n
70         %----- Update PRT and Step parameters -----
71         PRT = 0.05 + 0.90*(FEs/Max_FEs);
72         Step = 0.2 + 0.05*cos(4*pi*FEs/Max_FEs);
73         Migrant = pop(M(Im(j)),:);
74         %----- Leader selection: k -----
75         K = randperm(popsize,k);
76         [~,Ik] = mink(fit(K),2);
77         Leader = pop(K(Ik(1)),:);
78         if M(Im(j)) == K(Ik(2))
79             Leader = pop(K(Ik(2)),:);
80         end
81         %----- Moving process -----
82         nstep = Step*(1:N_jump)';
83         PRTVector = rand(N_jump,Dim) < PRT;
84         newpop = Migrant+(Leader-Migrant).*nstep.*PRTVector;
85         %----- Checking Boundary and Replaced Outsize Individuals -----
86         newpop(:,1) = max(newpop(:,1),Xmin);
87         newpop(:,1) = min(newpop(:,1),Xmax);
88         newpop(:,2) = max(newpop(:,2),Ymin);
89         newpop(:,2) = min(newpop(:,2),Ymax);
90         %----- SOMA Re-Evaluate Fitness Fuction -----
91         newfit = CostFunction(newpop);
92         FEs = FEs + N_jump;
93         %----- SOMA Accepting: Place Best Individual to Population-----
94         [min_fit,id] = min(newfit);
95         if min_fit <= fit(M(Im(j)))
96             pop(M(Im(j)),:) = newpop(id,:);
97             fit(M(Im(j))) = min_fit;
98         %----- SOMA Update Global_Leader -----
99         if min_fit < best_fit
100             best_fit = min_fit;
101             best_val = newpop(id,:);

```

```

102         end
103     end
104     %===Store and Display Results =====
105     try
106         Store_and_Display(filetxt,FEs,best_fit,best_val);
107         save(filemat)
108     catch
109         fprintf('Error while saving! Skipped this time. \n')
110     end
111     %-----
112 end % for j = 1 : n
113 end % while FEs+N_jump < Max_FEs
114 disp('DONE!')
115 diary off
116 %%%%%%%%%%%%%%%%%%%%%%%%%%%%%%%%%%%%%%%%%%%%%%%%%%%%%%%%%%%%%%%%%%%%%%%%%

```